Utrecht University

Master thesis

An optical dipole trap for transport of Rubidium-87 atoms

Author:
Sebastiaan Meyer Viol, Bsc

Supervisor:
Dr. Dries van Oosten
Ole Mussmann, Msc

September 16, 2014

Contents

CHAPTER 1

Introduction

Technological development and fundamental interest have stimulated researchers to look at light on the scale of the phenomena itself, namely the nanoscale. The relatively new field of nanoplasmonics investigates the interactions between light and metal structures at nanoscale. Plasmons are collective oscillations of the free electron density in a metal. At the interface between a metal and a dielectric, coupling between electromagnetic waves (e.g. light) and plasmons gives rise to surface plasmon polaritons [1]. What makes these surface plasmons so interesting is that they have yielded methods for guiding and localizing light at the nanoscale, below the wavelength of the light in free space [2].

These plasmons are not merely of fundamental interest but turn out to be of great practical use. Without being aware of the physics behind it, artists already used the effect of plasmons in the Middle ages. By applying gold colloids to the surfaces of stained glass windows of for example the Notre-Dame, surface plasmons are generated when light shines upon the windows [3]. This creates the remarkable colors observed. These features of plasmons may have amazed people in medieval times, they however stand pale in comparison to recent opportunities that have opened up with the understanding of the physics of plasmons. One possible application of plasmons is the the reduction of the physical thickness of photovoltaic absorber layers while keeping their optical thickness constant, leading to an increase in efficiency [2]. Plasmons have also been considered as a possible way to transmit information on computer chips, since plasmons can support very high frequencies [4]. A third possible application is the use of plasmons as a mean of high-resolution lithography and microscopy due to their extremely small wavelengths [5]. While many other applications may find their breakthrough in the coming years, in which a complete understanding of the underlying physics is lacking, research on plasmonics is of great interest.

A novel way to investigate the atom-light interaction in plasmonic nanostructures is by combining the field of nanoplasmonics with the field of ultracold atoms. This

field makes use of lasers and magnetic fields to cool, trap, and probe the atomic gases. This enables a high degree of control over the atoms, suitable to trap atoms in the near-field of plasmonic nanostructures and to look at the coupling and interactions. In our experiment we want to study the coupling between ^{87}Rb atoms and light close to a plasmonic nanostructure sample. To do this we place atoms close to the sample surface and trap them optically in the evanescent field of the nanoplasmonic structure. In this way we could for example investigate the interaction and the change in optical properties between a rubidium atom and a nanohole. An experimental setup is built to reproductively position the atoms close to the sample.

The setup globally works in the following way. First, ^{87}Rb atoms are trapped and cooled in a 2-D magneto-optical trap (MOT) inside a vacuum chamber. Afterwards the atoms are pushed into another vacuum chamber where a 3-D MOT will trap and cool the atoms further. The sample can not be placed under the atom cloud trapped by the 3-D MOT, as this would block one of the laser beams of the 3-D MOT. Therefore, an optical dipole trap (ODT) takes the atoms from the MOT and transports them in the horizontal direction towards the sample. To precisely position the atoms above the sample, a vertically aligned optical conveyor takes over the atoms and moves them down towards the sample surface [6]. The optical conveyor consists of two overlapping counterpropagating beams with the same wavelength, which trap the atoms in the anti-nodes of the standing wave that is created. By changing the frequency of one of the beams the position of the anti-nodes changes and hence the atoms can be moved down. Once the atoms are positioned close to the sample surface we want to be able to move them in the horizontal direction again. This can be done by translating the optical conveyor in the plane of the sample. The beams of the optical conveyor need to remain overlapped. The horizontal translation is performed by using two mirror galvanometers, which rotate by applying a current to them. Lenses are used to convert a change in angle to a change in position. In this way the counterpropagating beams of the optical conveyor can be horizontally translated while remaining overlapped [7].

This thesis will focus on the optical dipole trap which loads the atoms from the MOT and transports them to the sample. Chapter 2 will start by explaining the theory behind the trapping and cooling of neutral atoms. This will set the stage for the explanation of the working of the MOT. Finally, in this chapter the theory behind the ODT is explained in detail. Chapter 3 presents the experimental setup of the MOT. Chapter 4 presents the experimental setup of the ODT that has been built. With the ODT experiments have been performed to optimize loading and transport. The results of these experiments are presented in Chapter 5. Chapter 6 contains the conclusions of the experiments. Finally, in Chapter 7 recommendations for improvement of the ODT are given.

CHAPTER 2

Theory of laser cooling and trapping of neutral atoms

The main focus of this thesis is the loading and transport of ^{87}Rb atoms with an optical dipole trap (ODT). The ODT can only trap cold atoms [8]. Therefore, the atoms first need to be cooled. Neutral atoms can conveniently be cooled down to the microkelvin regime by using a magneto-optical trap (MOT) [9]. The MOT makes use of both a magnetic field gradient and laser beams to cool and trap the atoms. Afterwards, the atoms can be loaded into the ODT, and transported towards the sample. This chapter contains the theoretical concepts of the MOT and the ODT.

The chapter is divided into three sections. Section 2.1 explains the concept of the laser cooling technique of neutral atoms that we use in the MOT. The technique that is used is called Doppler cooling. The optical field of the laser creates a velocity-dependent force on the atoms which will be derived in this section. Apart from cooling the atoms, a MOT also traps the atoms. Section 2.2 explains how the MOT uses a magnetic field to create a position-dependent force on the atoms which traps them. Once a cloud of cold atoms is obtained by the MOT, the ODT can load the atoms and transport them. The ODT makes use of the optical dipole force to trap the atoms. Three important properties of the ODT are the trap depth, the trap frequency and the scattering rate. These properties will be derived in Section 2.3.

2.1 Doppler cooling

The temperature of an ensemble of atoms is equivalent to their average kinetic energy. Therefore the atoms can be cooled by applying a force that decreases the velocity. The force should be velocity dependent and in opposite direction of the movement of the atoms in order to slow them down. In other words, it should be a friction. Doppler cooling is a widely used technique [8,10] that uses lasers for this purpose. To understand the mechanism of Doppler cooling we will first explain the structure of a two-level atom.

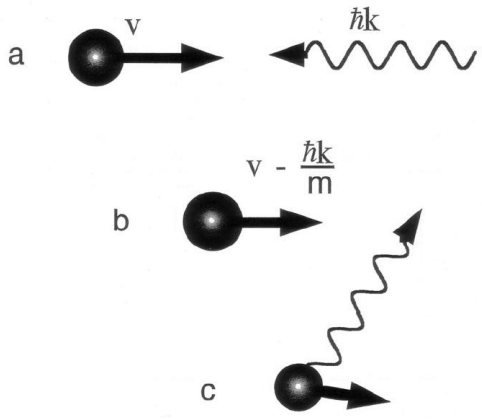

Figure 2.1: Process of absorption and emission of a photon by an atom. a) A photon collides with an atom, and gets absorbed. b) This causes a momentum change of the atom. c) The atom then emits the photon in a random direction. [11]

The two-level atom consists of two energy levels, that we will call the ground state and the excited state. The energy difference between the ground state and the excited state is $\hbar\omega_0$, where ω_0 is called the resonance frequency. The atom can absorb or emit a photon if the frequency of the photon is equal to this resonance frequency. If the atom absorbs a photon with momentum $\mathbf{p} = \hbar\mathbf{k}$ (Figure 2.1 a), an electron is excited from the ground state to the excited state and the velocity of the atom is reduced by $\mathbf{v} = \hbar\mathbf{k}/m$ (Figure 2.1 b). Eventually, the atom will spontaneously emit the photon in a random direction (Figure 2.1 c). The atom again gains the momentum of the photon.

If a laser with frequency ω_{L} and intensity I, illuminates the atom, the total force this laser exerts on the atom in its reference frame is

$$\mathbf{F} = \frac{d\mathbf{p}}{dt} = \hbar\mathbf{k}\Gamma_{\mathrm{sc}}, \tag{2.1}$$

where Γ_{sc} is the scattering rate and $\hbar\mathbf{k}$ is the momentum transfer of each photon. The scattering rate can be derived from the optical Bloch equations [8]. For an atom at rest this scattering rate is

$$\Gamma_{\mathrm{sc}} = \left(\frac{\gamma}{2}\right) \frac{s}{1 + s + 4(\Delta/\gamma)^2}. \tag{2.2}$$

In this equation γ is the natural linewidth of the transition, and $1/\gamma$ is the lifetime of the excited state. The saturation parameter $s = I/I_{\mathrm{sat}}$, and $I_{\mathrm{sat}} = \frac{\pi hc\gamma}{3\lambda^3}$ is the saturation intensity of the beam which depends on the wavelength λ. The detuning $\Delta = (\omega_{\mathrm{L}} - \omega_0)$ is the frequency difference between the laser and the resonance frequency.

From Equation (2.2) two important conclusions can be drawn. First, the scattering rate and thus the force is maximized for $\Delta = 0$. This means that the force on the atoms will be largest if the frequency of the laser is equal to the resonance frequency. Second, by increasing the intensity of the laser beam the scattering rate also increases. The scattering rate is plotted in Figure 2.2 against the saturation parameter. If $I \gg I_{sat}$,

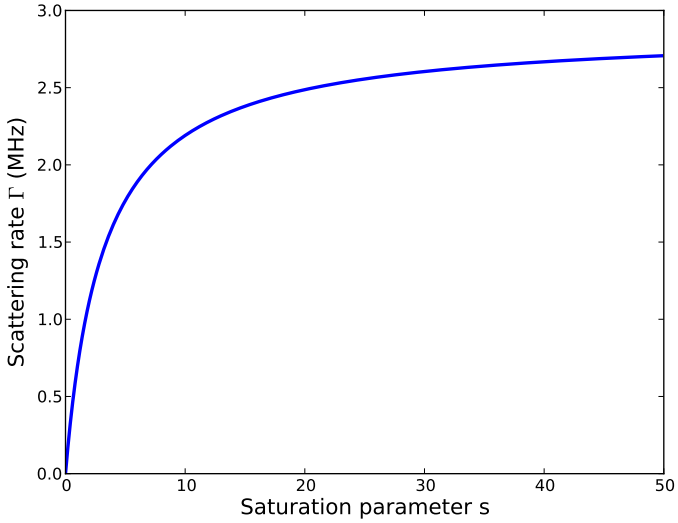

Figure 2.2: The scattering rate in MOL plotted against the saturation parameters $s = I/I_{\text{sat}}$. The detuning $\Delta = 8.4$ MHz is also the detuning used to generate a 3-D MOT. The natural linewidth $\gamma = 2\pi \cdot 6$ MHz, which is the decay rate of ^{87}Rb.

s becomes much larger than $1 + 4(\Delta/\gamma)^2$ in the denominator. The scattering rate eventually saturates with a maximum of $\gamma/2$. The force then becomes $\hbar\mathbf{k}\gamma/2$. This saturation is caused by the fact that stimulated emission limits the population of the upper state to 50%.

Doppler cooling makes use of a laser beam whose frequency is detuned slightly below (red-detuned) the electronic transition of the atom such that $\omega_{\text{L}} = \omega_0 + \Delta$, with $\Delta < 0$. The atom experiences the frequency of the laser in its frame of reference with a Doppler shift $\omega_{\text{D}} = -\mathbf{k} \cdot \mathbf{v}$. The frequency of the laser light in the frame of reference of the atom then is $\omega'_{\text{L}} = \omega_{\text{L}} - \omega_{\text{D}} = \omega_{\text{L}} + \mathbf{k} \cdot \mathbf{v} = \omega_0 + \Delta + \mathbf{k} \cdot \mathbf{v}$. This means that if the detuning Δ is equal but opposite to the Doppler shift $\omega_{\text{D}} = \mathbf{k} \cdot \mathbf{v}$, the atom will see the laser beam as emitting light at resonance frequency ω_0. From Equation (2.2) it follows that the atom then has the highest probability of absorbing a photon. The Doppler shift is equal in magnitude but opposite in sign to the detuning of the laser when the atom moves towards the laser beam. Therefore an atom moving towards the laser beam has the highest chance to absorb a photon. If the atom absorbs a photon it will be slowed down due to conservation of momentum. The atom spontaneously re-emits the photon but in a random direction. Therefore after many scattering events, the net effect of momentum gain due to spontaneous emission is zero. To conclude the atoms are slowed down in one direction by the laser beam.

If we now have two counterpropagating laser beams with a slight red detuning to resonance illuminating a cloud of atoms, the atoms are slowed down and thus cooled in both directions of propagation of the laser beams. This model can be extended to a

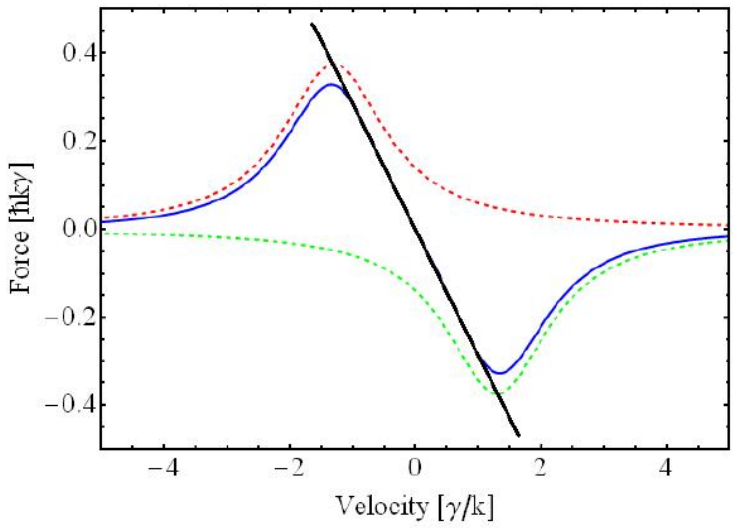

Figure 2.3: The force working on the neutral atoms plotted against the velocity of the atoms, with detuning $\Delta = -1.3$, and saturation $I/I_0 = 3$. The red curve is the force from the beam from the left, the green curve is the force from the beam from the right, and the blue curve is the total force. The force is in opposite direction of the velocity, hereby decelerating the atoms. [12]

2-D or 3-D model by directing two counterpropagating laser beams on the atom cloud for each dimension. The laser cooling technique that makes use of this mechanism is called optical molasses (MOL). It is important to note that MOL only cools and does not trap the atoms as there is no force that drives the atoms towards a trapping centre.

The force that MOL exerts on the atom in one dimension, if the intensity and detuning of both laser beams is equal, is [8]

$$\mathbf{F}_{\mathrm{MOL}} = \mathbf{F}_+ + \mathbf{F}_- = \frac{\hbar \mathbf{k} \gamma}{2} \left(\frac{s}{1 + s + 4((\Delta - \omega_{\mathrm{D}}))/\gamma)^2} - \frac{s}{1 + s + 4((\Delta + \omega_{\mathrm{D}})/\gamma)^2} \right). \tag{2.3}$$

The force is plotted against the velocity of the atoms in Figure 2.3. This graph shows that the force is in opposite direction to the velocity of atoms. In the regime where the atoms are slow, the relation between the force and the velocity is linear. An approximation can be made of Equation 2.3 in the regime where $|\mathbf{v}| \ll \gamma/\mathbf{k}$. In this regime then $\omega_{\mathrm{D}} = \mathbf{k} \cdot \mathbf{v} \ll \gamma$ and Equation 2.3 becomes [8]

$$\mathbf{F}_{\mathrm{MOL}} \simeq \frac{8\hbar k^2 \Delta s}{\gamma(1 + s + 4(\Delta/\gamma)^2)^2} \mathbf{v} \equiv -\beta \mathbf{v}. \tag{2.4}$$

where β is the frictional constant.

The cooling that can be achieved by MOL is limited by the heating due to the random recoil of atoms when emitting a photon. The minimum temperature of the atoms that

can be achieved by Doppler cooling is the Doppler cooling limit. The Doppler cooling limit is [8]

$$T_D = \frac{\hbar\gamma}{2k_b}, \tag{2.5}$$

For ^{87}Rb, the natural linewidth $\gamma = 2\pi \cdot 6$ MHz [13]. The calculated theoretical Doppler temperature limit with MOL in the framework of the above described model is $T_D = 146\mu$K. While the neutral atoms will be cooled by Doppler cooling, a magnetic field gradient is needed to trap the atoms. The next section will explain the magnetic trapping mechanism.

2.2 Magneto-optical trap

The MOT is a device that uses laser cooling with magneto-optical trapping to produce samples of cold trapped neutral atoms [9]. In a MOT two (2-D MOT) or three (3-D MOT) pairs of counterpropagating laser beams illuminate a cloud of atoms to cause Doppler cooling. Apart from Doppler cooling the MOT uses a magnetic field to trap the atoms. To understand the trapping mechanism we first need to look at the properties of the atom.

Let us consider an atom of the simplest level structure with hyperfine components F = 0 and F = 1 for the ground and excited state. Each of the hyperfine levels contains 2F + 1 magnetic sublevels that determine the angular distribution of the electron wave function. The excited state thus has three magnetic sublevels with magnetic quantum number $m_F = 0, \pm 1$. In the absence of a magnetic field these three sublevels are degenerate and thus have the same energy. However in the presence of a magnetic field the energy of these sublevels is shifted by [14]

$$\Delta E_{m_\mathrm{F}} = g_\mathrm{F}\mu_\mathrm{B}B(z)m_\mathrm{F}. \tag{2.6}$$

In this formula, g_F is the Landé factor, and $\mu_\mathrm{B} = e\hbar/2m_\mathrm{e}$ is the Bohr magneton which includes the elementary charge e, and the mass of an electron m_e. The effect of the splitting of the energy of the sublevels due to a magnetic field is called the Zeeman effect.

In a MOT the counter-propagating beams have opposite circular polarization σ_+ and σ_-. Due to the conservation of angular momentum the σ_- polarized light can only cause a transition in which the change in magnetic spin quantum number is $\Delta m = -1$, while the σ_+ polarized light can only cause a transition in which the change is $\Delta m = +1$. Figure 2.4 shows the dependence of the energy levels on the position of the atom in a MOT. In the MOT a magnetic field gradient is applied with $B = 0$ at $z = 0$. The energy levels of the excited state are shifted due to the Zeeman effect. The beam with σ_+ polarization comes from the left, while the beam with σ_- polarization comes from the right. The laser is detuned by Δ to the resonance frequency of the atom. If an atom is located at position 1, the Zeeman splitting will cause the $m_F = 1$ transition to be shifted closer to resonance. As this transition is excited by the σ_+ polarized light, more

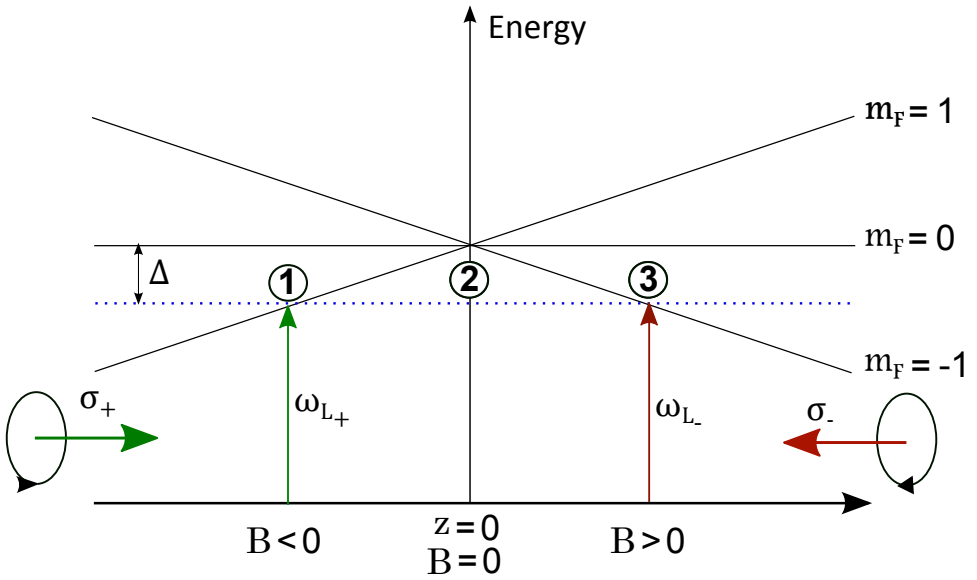

Figure 2.4: In this graph the energy of the ground state and excited state of an atom in a MOT is plotted against the z-coordinate. Along the z-axis two counterpropagating beams with polarization σ_+ and σ_- illuminate the atom. The beams are detuned by Δ to the resonance frequency of the atom. There is a magnetic field gradient along the z-axis, with $B = 0$ at $z = 0$. Due to the Zeeman effect the energy levels are split. An atom at position 1 is most likely to be scattered by the laser beam coming from the left, while an atom at position 3 is most likely to be scattered by a laser beam coming from the right. At position 2 the atom has an equal chance to be scattered by the laser beam coming from the left, as by the laser beam coming from the right.

atoms will be scattered by the beam coming from the left than by the beam coming from the right. The result is a net impulse towards the right. The opposite holds for an atom located at position 3. Here the $m_F = -1$ transition is closer to resonance. Therefore at this position we have a net impulse towards the left. In the centre of the trap at position 2, the magnetic field is zero and there is no energy shift of the excited states. The beams both have the same scattering rate here, and there is no net impulse experienced by the atoms. This results in atoms being trapped at and around $z = 0$. If the model is extended to two orthogonal pairs of counterpropagating beams along with a magnetic field gradient in both directions we have a 2-D MOT. Three orthogonal pairs of counterpropagating beams along with a magnetic field gradient in all three directions make a 3-D MOT.

The force working on the atoms in a MOT can be modified from Equation (2.3) to include the effect of the magnetic field gradient. The force in one dimension is

$$\mathbf{F}_{\mathrm{MOT}} = \mathbf{F}_+ + \mathbf{F}_- = \frac{\hbar \mathbf{k} \gamma}{2} \left(\frac{s}{1 + s + 4((\Delta - \omega_D + \omega_Z)/\gamma)^2} - \frac{s}{1 + s + 4((\Delta + \omega_D - \omega_Z)/\gamma)^2} \right), \tag{2.7}$$

where $\omega_Z = \mu' B(z)/\hbar$ is the Zeeman shift. The effective magnetic moment of the transition $\mu' = (g_{\mathrm{F_e}} m_{\mathrm{F_e}} - g_{\mathrm{F_g}} m_{\mathrm{F_g}})\mu_{\mathrm{B}}$, where subscript g and e stand for the ground state and the excited state. What is achieved with the extra magnetic Zeeman term in the force equation is that the force not only depends on the *velocity* of the atoms, but also on the *position*. Again, a limiting case of the derived formula can provide us with additional insight into the force generated by the magnetic field. For small atom velocities and small displacements from the trap centre, $\omega_{\mathrm{D}} \ll \gamma$ and $\omega_{\mathrm{Z}} \ll \gamma$, the force working on the atoms can be approximated as [8]:

$$\mathbf{F}_{\mathrm{MOT}} = -\beta \mathbf{v} - \kappa \mathbf{z}, \tag{2.8}$$

with $\kappa = \mu' \beta (dB/dz)/\hbar k$ the spring constant. The restoring force now has a different direction for positive than for negative z, creating a trap around $z = 0$.

So far we have described the 2-level system that traps and cools the atoms. Alkali atoms like rubidium however are more complex multi-level systems. The magnetic field creates a hyperfine structure for ^{87}Rb as depicted in Figure 2.5. Appendix A gives a more thorough explanation of the splitting of the rubidium energy levels. The lasers that cool and trap the atoms are called the **cooling** lasers. The cooling and trapping depends on the presence of a closed transition for the cycle of absorption and spontaneous emission. The transition that is used for cooling the atoms is the $F = 1 \rightarrow F^{'} = 3$ transition. The frequency of the cooling beam is slightly red-detuned to this transition with a detuning Δ. Due to the level splitting a second ground state is formed, the $F = 0$ state. Because the linewidth of the MOT lasers is much smaller than the splitting between the levels, the atoms will also be pumped to this second ground state. Atoms in this ground state however are not affected by the cooling laser, so atoms pumped to this ground state will be lost. This means the system would lose atoms to cool and would therefore be less effective. To avoid this problem, a second laser is used which we call the **repump** laser. This laser has a different frequency than the cooling laser and can excite the atoms from the second ground state ($F = 0$) to the excited state ($F = 2^{'}$). From here they can decay to the $F = 1$ ground state that participates in the cooling transition.

2.3 Optical dipole trap

Optical dipole traps (ODT's) are far-off resonant traps that rely on the interaction between the induced atomic electric dipole moment and far-detuned light. A large detuning is used to achieve a low spontaneous scattering rate. The trapping time of the ODT is in the order of seconds. Section 2.3.1 will start with a classical description of the optical dipole trap. To describe the ODT of alkali-atoms like rubidium, a quantum mechanical description is needed. The quantum mechanical model will be explained in Section 2.3.2. In section 2.3.3 we will use the quantum mechanical model to describe the rubidium ODT. Section 2.3.4 will explain the different types of ODT's. In this section also the trapping depth, trapping frequency, and scattering rate will be quantified for rubidium in the ODT we build.

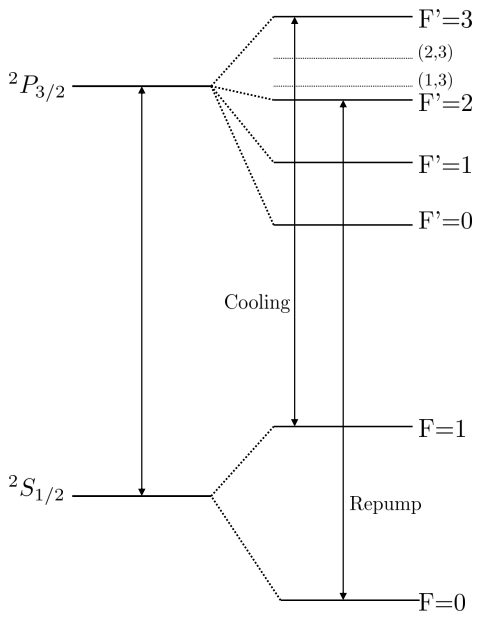

Figure 2.5: ^{87}Rb line spectrum including cooling and repump transition. The (1,3) and (2,3) cross-over transition are generated by the saturation absorption spectroscopy explained in Appendix B.

2.3.1 Classical harmonic oscillator model

To build an ODT, a laser beam which has an intensity gradient in the light field, is focused on a cloud of cold atoms. Due to the presence of the electric field of the laser, the positive and negative charges in the atom experience opposing forces. This causes separation of the charges. This charge separation induces an atomic dipole moment. The interaction of this atomic dipole moment with the intensity gradient of the laser beam creates an optical dipole force. The force which is generated is conservative. That means the force can be written as the negative gradient of the potential. The first step is finding an expression for the potential of the ODT. From this the optical dipole force working on the atom can be derived. A second important quantity that will be derived is the scattering rate. The scattering rate is preferably low in an ODT as scattering leads to heating. In this section these quantities are derived with a classical harmonic oscillator model.

To start the quantitative analysis, suppose a laser beam illuminates an atom. The electric field is $\mathbf{E}(\mathbf{r},t) = \hat{\mathbf{e}}E(\mathbf{r})\exp(-i\omega t)$. This electric field induces an atomic dipole moment $\mathbf{p}(\mathbf{r},t) = \hat{\mathbf{e}}p(\mathbf{r})\exp(-i\omega t)$ due to charge separation, oscillating at the driving frequency ω. The unit polarization vector is $\hat{\mathbf{e}}$, and the amplitude of the electric field and dipole moment are E and p. The atomic dipole moment and the electric field are related by $\mathbf{p} = \alpha(\omega)\mathbf{E}$, with α being the complex polarizability. The interaction

potential of the dipole moment is [10]

$$U_{\text{dip}} = -\frac{1}{2}\langle \mathbf{pE} \rangle = -\frac{1}{2\epsilon_0 c}\text{Re}[\alpha] I(\mathbf{r}),\ I(\mathbf{r}) = \frac{\epsilon_0 c}{2}|E|^2, \tag{2.9}$$

with I the field intensity, $\langle . \rangle$ the time average over many oscillations, c is the speed of light, and ϵ_0 is the vacuum permittivity. The factor $\frac{1}{2}$ arises from the fact that the dipole moment is induced by the field and is not permanently there. The real part of the polarizability is the in-phase component of the dipole oscillation. The imaginary part leads to absorption of power from the driving field [10]. The conservative electric dipole force can now be written as the gradient of the dipole potential

$$F_{\text{dip}}(\mathbf{r}) = -\nabla U_{\text{dip}}(\mathbf{r}) = \frac{1}{2\epsilon_0 c}\text{Re}[\alpha]\nabla I(\mathbf{r}). \tag{2.10}$$

As long as the polarizability is positive, the force is directed towards the focus of the laser, where the intensity is highest.

The second important quantity, the scattering rate, is proportional to the amount of power that is absorbed from the driving field. The imaginary part of the polarizability is the component that is out of phase with the driving field and hereby causing absorption. The absorbed power is the change in dipole potential over time [10]

$$P_{\text{abs}} = \left| \frac{dU_{\text{dip}}}{dt} \right| = \left\langle \frac{d\mathbf{p}}{dt}\mathbf{E} \right\rangle = 2\omega \text{Im}[pE^\star] = \frac{\omega}{\epsilon_0 c}\text{Im}[\alpha] I(\mathbf{r}). \tag{2.11}$$

To get the scattering rate this power needs to be divided by the energy of one photon. With $\hbar\omega$ the energy of a photon, the scattering rate is

$$\Gamma_{\text{sc}}(\mathbf{r}) = \frac{P_{\text{abs}}}{\hbar\omega} = \frac{1}{\hbar\epsilon_0 c}\text{Im}[\alpha] I(\mathbf{r}). \tag{2.12}$$

The dipole potential and the scattering rate are the two main quantities of an ODT. These quantities are dependent upon the position dependent intensity of the beam $I(\mathbf{r})$ and the polarizability $\alpha(\omega)$. In Section 2.3.4 we will come back to the intensity of the beam we use. To derive the polarizability one can either use a classical Lorentz-oscillator approach or a semiclassical approach. In this section first a classical Lorentz model will be used to derive the polarizability. This model is simple and very useful to gain physical insight. With a small modification the model can be extended to a semi"classical model.

In the classical model an electron is bound elastically to the atom core, oscillating with eigenfrequency ω_0. The nucleus of the atom is assumed to have a much larger mass than the electron. The electron can be treated as being connected by a spring to the heavy nucleus. The driving force of oscillating movement is the electric field of the laser. The classical equation of motion of an electron bound elastically to the atom core is [15]

$$F = m_e \ddot{x}(t) = -m_e \Gamma \dot{x}(t) - m_e {\omega_0}^2 x(t) - eE(t). \tag{2.13}$$

The first term on the right side is a damping term, with Γ the classical damping rate and m_e the mass of the electron. It represents the rate at which the polarization will decay after the electric field has been removed. The second term on the right side is the restoring force of the electron. The electron is bound to the nucleus and oscillates at resonance frequency ω_0. This force can be seen as a spring force with spring constant ω_0^2. The third term on the right side is the driving force originating from the electric field $E(t)$. It includes the electronic charge e.

By inserting $E(t) = E_0 \exp(-i\omega t)$ and $x(t) = x_0 \exp(-i\omega t)$ this second order differential equation can be solved, giving

$$x_0 = \frac{-eE_0}{m_e} \frac{1}{{\omega_0}^2 - \omega^2 - i\omega\Gamma}. \tag{2.14}$$

Making use of the relation $p(t) = -ex(t) = \alpha E(t)$ a solution for the polarizability α can be found

$$\alpha(\omega) = \frac{-e^2}{m_e} \frac{1}{{\omega_0}^2 - \omega^2 - i\omega\Gamma}. \tag{2.15}$$

The on-resonance damping rate Γ which results from radiative energy loss in the classical harmonic oscillator approach is [15]

$$\Gamma = \frac{e^2\omega_0^2}{6\pi\epsilon_0 m_e c^3}. \tag{2.16}$$

To determine the polarizability with a semiclassical approach the atom is considered as a two-level quantum system with a classical radiation field. When saturation effects can be neglected, the semiclassical calculation yields exactly the same results as the classical calculation with one modification, the damping rate Γ. ODT's operate at large detunings. Therefore the atom is mostly kept in the ground state as scattering is minimized, and saturation effects can be neglected. The only necessary modification in the semiclassical approach then is the damping rate, which now becomes [10],

$$\Gamma = \frac{\omega_0^3}{3\pi\epsilon_0\hbar c^3} |\langle \mathrm{e}|\mathbf{d}|\mathrm{g}\rangle|^2, \tag{2.17}$$

where $|\langle \mathrm{e}|\mathbf{d}|\mathrm{g}\rangle|$ is the dipole matrix element between the ground and the excited state.

With the polarizability α derived, the final expressions for the dipole potential and the scattering rate can be found. By separating the Real part and the Imaginary part of the polarizability and inserting it into Equation (2.9) and (2.12), we find that with a classical approach the dipole potentials is

$$U_{\mathrm{dip}}(\mathbf{r}) = -\frac{3\pi c^2}{2{\omega_0}^3} \left(\frac{\Gamma}{\omega_0 - \omega} + \frac{\Gamma}{\omega_0 + \omega} \right) I(\mathbf{r}), \tag{2.18}$$

and the scattering rate is

$$\Gamma_{\mathrm{sc}}(\mathbf{r}) = \frac{3\pi c^2}{2\hbar{\omega_0}^3} \left(\frac{\omega}{\omega_0} \right)^3 \left(\frac{\Gamma}{\omega_0 - \omega} + \frac{\Gamma}{\omega_0 + \omega} \right)^2 I(\mathbf{r}). \tag{2.19}$$

To understand the physics of ODT's, these equations can be simplified by the rotating wave approximation [16]. This approximation is valid when the frequency of the beam is relatively close to the resonance frequency of the atomic transition, thus $\omega/\omega_0 \approx 1$. The second term in Equation 2.18 and 2.19 becomes much smaller than the first term, because the detuning $\Delta = \omega_0 - \omega \ll \omega_0 + \omega$, and can therefore be neglected. Note that this approximation will only be used to understand the physics behind ODT, because the ODT used in the experiment is relatively far from resonance. The dipole potential and scattering rate with the rotating wave approximation become

$$U_{\mathrm{dip}}(\mathbf{r}) = \frac{3\pi\Gamma c^2}{2{\omega_0}^3\Delta} I(\mathbf{r}), \tag{2.20}$$

and

$$\Gamma_{\mathrm{sc}}(\mathbf{r}) = \frac{3\pi c^2}{2\hbar^3\omega_0^3}\left(\frac{\Gamma}{\Delta}\right)^2 I(\mathbf{r}). \tag{2.21}$$

From these two equations two important conclusions can be drawn. First of all, the sign of the dipole potential depends on the detuning $\Delta = \omega - \omega_0$. Red detuning ($\Delta < 0$) causes the dipole potential to be negative. The potential minimum is found where the intensity of the beam is maximum. This explains why the atoms can be trapped at the center of the focus in a red-detuned optical dipole trap. Blue detuned traps ($\Delta > 0$) have a positive potential and minima can be found at minimum intensity of the beam, making this a whole different type of trap. The optical dipole trap which will be used in the experiment is a red-detuned trap.

From Equation 2.20 and 2.21 a second important conclusion can be drawn. The scattering rate scales with I/Δ^2, while the dipole potential only scales with I/Δ. To keep the scattering rate low, a large detuning can be applied. In order to compensate for the decrease in dipole potential, the intensity of the laser beam can be increased. This means that in an ODT a high intensity laser is needed with a large detuning. The laser intensity used in the experiment is 10.2 W. The wavelength of the laser is 1070.6 nm, which corresponds to a frequency of 280 THz. The resonance frequency of ^{87}Rb is 384 THz. This means the laser is detuned 104 THz to the red of the ^{87}Rb resonance frequency.

2.3.2 Multi-level quantum mechanical model

The classical harmonic oscillator model is not able to describe the trapping of atoms which have a complex sub-structure in the electronic transition. As alkali atoms like rubidium have a complex sub-structure a quantum mechanical approach is needed to describe the dipole potential and scattering rate of the rubidium ODT.

The effect of the far-detuned light field on the atom can be treated as a second order perturbation in the electric field. From perturbation theory it follows that the interaction of the atom with the light field leads for the non-degenerate atomic states $|i\rangle$ to an energy shift ΔE_i [10]

$$\Delta E_i = \sum_{i \neq j} \frac{|\langle j|H_{\mathrm{AL}}|i\rangle|^2}{\epsilon_i - \epsilon_j}, \tag{2.22}$$

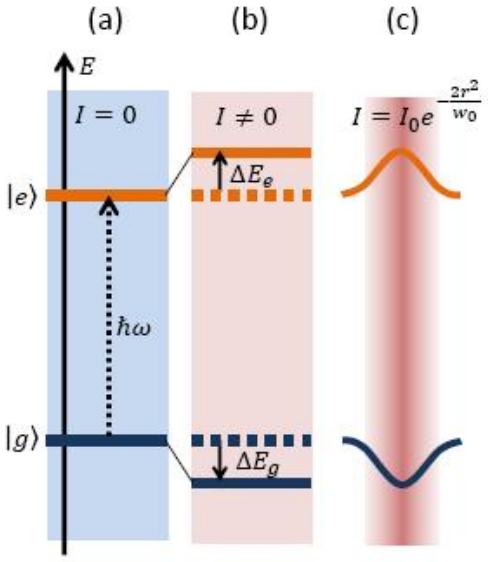

Figure 2.6: Energy transition scheme showing the ground state and the excited state of a 2-level atom. a) Energy transition of the atom. b) The red-detuned laser beam shifts the ground state and excited state energy. c) The energy change of the ground state and the excited state of an atom illuminated by a Gaussian laser beam. [10]

with ϵ_i the unperturbed energy of the i-th state. In this formula $H_{\mathrm{AL}} = \mathbf{d} \cdot \mathbf{E}$ is the perturbation from the unperturbed state, and $\mathbf{d}$ is the dipole operator.

In a two-level system in the ground state, the field energy due to the laser is $n\hbar\omega_L$, with n the number of photons. The energy of the atom is 0, which gives a total energy $\epsilon_{\mathrm{g}} = n\hbar\omega_{\mathrm{L}}$. In the excited state a photon is absorbed, making the energy of the atom $\hbar\omega_0$ so the total energy is $\epsilon_{\mathrm{e}} = \hbar\omega_0 + (n-1)\hbar\omega_{\mathrm{L}}$. Now for a two-level atom, where the incident light is represented by an oscillating electric field, Equation 2.22 reduces to [17]

$$\Delta E = \pm \frac{|\langle \mathrm{e}|\mathbf{d}|\mathrm{g}\rangle|^2}{\hbar\Delta}|E|^2 = \pm \frac{3\pi c^2}{2\omega_0^3}\frac{\Gamma}{\Delta} I(\mathbf{r}), \tag{2.23}$$

where g and e are the ground and excited state of the atom. The minus sign gives the energy shift of the ground state, while the plus sign gives the energy shift of the excited state. Equation 2.17 and the relation $I = 2\epsilon_0 c|E|^2$ have been used to substitute the dipole matrix element with the damping rate. The energy shift ΔE is dependent upon the intensity of the laser beam. For a Gaussian laser beam the change in energy therefore depends on the radial and axial coordinate. The energy shift is the largest in the centre of the beam and in the beam focus. Figure 2.6 shows the energy shift of the energy levels of a 2-level atom created by a Gaussian laser beam.

The derivation of the energy shift for a multi-level atom is more complex. All possible dipole matrix elements $d_{ij} = \langle e_i|\mathbf{d}|g_j\rangle$, for transitions between the ground state and exited state have to be taken into account. For given transitions these matrix

elements become

$$d_{ij} = c_{ij}||d||, \tag{2.24}$$

where $||d||$ is a reduced matrix element and c_{ij} is the transition or Clebsch-Gordan coefficient. This transition coefficient c_{ij} takes into account the coupling strength between the sublevels i and j of the electronic ground and excited state. In this thesis we will not go into detail into how this coefficient can be derived. The resulting energy shift of the electronic ground state for a multi-level atom requires a slight modification of Equation 2.23, namely

$$\Delta E_i = \frac{3\pi c^2 \Gamma}{2\omega_0^3} I(\mathbf{r}) \sum_j \frac{c_{ij}^2}{\Delta_{ij}}, \tag{2.25}$$

which includes a summed over all electronically excited states. For the calculation of the state-dependent ground-state dipole potential one thus has to take into account the contribution of all coupled excited states. Each transition has a line strength c_{ij} and a detuning Δ_{ij}.

2.3.3 An optical dipole trap for ^{87}Rb

From Equation 2.25 the dipole potential for rubidium can be derived. Appendix A gives the level scheme for ^{87}Rb. ^{87}Rb contains two relevant transitions, namely the D1 and D2 transition. The total dipole potential for ^{87}Rb is [13]

$$U_{\text{dip}}(\mathbf{r}) = \frac{\pi c^2 \Gamma}{2\omega_0^3} \left(\frac{1 - P g_F m_F}{\Delta_1} + \frac{2 + P g_F m_F}{\Delta_2} \right) I(\mathbf{r}), \tag{2.26}$$

and the scattering rate is

$$\Gamma_{\text{scat}}(\mathbf{r}) = \frac{\Gamma}{\hbar\Delta} U_{\text{dip}} = \frac{\pi c^2 \Gamma^2}{2\hbar\omega_0^3} \left(\frac{1 - P g_f m_F}{\Delta_1^2} + \frac{2 + P g_f m_F}{\Delta_2^2} \right) I(\mathbf{r}), \tag{2.27}$$

In this equation Δ_i is the detuning of the D_i transition. The polarization of the light $P = \pm 1$ for $\sigma^{\pm}$ polarised light. The magnetic quantum number is m_F. The Landé factor is [13]

$$g_F = g_J \frac{F(F+1) - I(I+1) + J(J+1)}{2F(F+1)}, \tag{2.28}$$

with

$$g_J = 1 + \frac{J(J+1) + S(S+1) - L(L+1)}{2J(J+1)}, \tag{2.29}$$

where F is the hyperfine level quantum number, I is the nuclear spin, S is the electron spin quantum number, L is the electron orbital quantum number, and J is the total angular momentum quantum number. In Appendix A an explanation of the quantum numbers for the ^{87}Rb atom can be found. The ground state of ^{87}Rb is the $^2S_{1/2}$ state, which means $g_J = 2$. To calculate the dipole potential and the scattering rate we need the intensity of the laser beam in the focus. To calculate this intensity at focus we will first look at the type of ODT that is used.

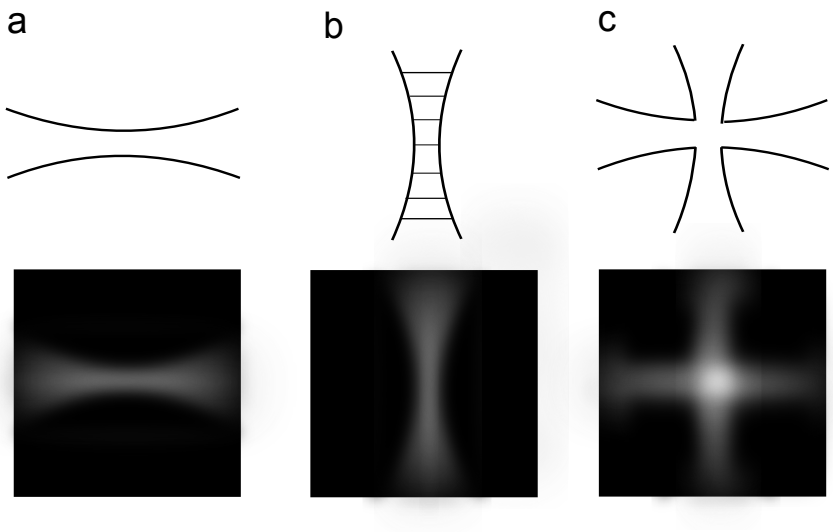

Figure 2.7: Different types of optical dipole traps. a) The focused beam trap, b) the standing wave trap and c) the crossed-beam trap.

2.3.4 Types of optical dipole traps

In this section the different types of laser configurations in ODT's are explained. Since the first ODT was created, three different kind of trap geometries based on Gaussian beams have been generated. The first one is the focused-beam trap, which consists of a single Gaussian beam (Figure 2.7 a). The second ODT configuration is a standing wave trap, where atoms are axially confined in the antinodes of the standing wave (Figure 2.7 b). A third ODT configuration is the crossed-beam trap (Figure 2.7 c), consisting of two beams which cross each other at the focus. In this section focused beam traps and crossed-beam trap will be explained. The focused beam trap is implemented in the setup. If the density of atoms trapped in the focused beam trap turns out to be insufficient for the final experiment we may decide to implement a crossed-beam which increases the density.

Focused beam optical dipole trap

The simplest way to create an optical dipole trap with three-dimensional spatial confinement is a focused Gaussian laser beam tuned far below resonance. The spatial intensity distribution of a focused Gaussian beam propagating along the z-axis with power P is [15]

$$I_{\text{circ}}(r,z) = \frac{2P}{\pi w^2(z)} \exp\left(\frac{-2r^2}{w^2(z)}\right), \tag{2.30}$$

with r denoting the radial coordinate, and $w(z)$ the $1/e^2$ radius of the beam. The $1/e^2$ radius of the beam also depends upon the axial coordinate z via

$$w(z) = w_0\sqrt{1+\left(\frac{z}{z_R}\right)^2}. \tag{2.31}$$

Here $z_R = \pi w_0^2/\lambda$ is the Rayleigh length, and w_0 is the radius of the beam at the focus. z_r is bigger than w_0 by a factor $\pi w_0/\lambda$. This means the atoms are more confined in the radial direction than in the longitudinal direction, as the intensity gradient is larger along the radial direction.

Now that we know the intensity distribution we also know the optical potential of the focused beam trap using Equation 2.26. The trap depth is defined as $U_0 = |U(r = 0, z = 0)|$, the magnitude of the trapping potential at the centre of the trap. To determine the trapping frequency in the radial and axial direction we approximate the dipole potential by a cylindrically symmetric harmonic oscillator. This approximation can be made if the thermal energy of the atomic ensemble is much lower than the potential trap depth. As the thermal energy in our atomic ensemble is in the order of 100 μK, while the trap depth is in the order of 1 mK this approximation can be made. The optical potential now becomes [10]

$$U_{\text{circ}}(r, z) \simeq -U_0 \left(1 - 2\left(\frac{r}{w_0}\right)^2 - \left(\frac{z}{z_R}\right)^2\right) = -U_0 + \frac{1}{2}m\omega_r^2 r^2 + \frac{1}{2}m\omega_z^2 z^2, \tag{2.32}$$

where ω_r and ω_z are the trapping frequencies in the radial and axial direction

$$\omega_r = \sqrt{\frac{4U_0}{mw_0^2}}, \tag{2.33}$$

$$\omega_z = \sqrt{\frac{2U_0}{mz_0^2}}. \tag{2.34}$$

In the experiment the beam shape is not circular but elliptical. To implement this in the theory some minor modifications need to be made to Equation 2.30 and 2.32. For an elliptical beam the waists in radial x and y direction are different so they will be defined as $w_x(z)$ and $w_y(z)$. The cross-section of the beam changes and the intensity profile now is

$$I_{\text{ellip}}(r, z) = \frac{2P}{\pi w_x w_y} \exp\left(\frac{-2x^2}{w_x^2(z)} + \frac{-2y^2}{w_y^2(z)}\right). \tag{2.35}$$

The harmonic approximation of the trapping potential is

$$\begin{aligned} U_{\text{ellip}}(r, z) &\simeq -U_0 \left(1 - \frac{2x^2}{w_x^2} - \frac{2y^2}{w_y^2} - \frac{1}{2}z^2\left(\frac{1}{z_{R_x}^2} + \frac{1}{z_{R_y}^2}\right)\right) \\ &= -U_0 + \frac{1}{2}m\omega_x^2 x^2 + \frac{1}{2}m\omega_y^2 y^2 + \frac{1}{2}m\omega_z^2 z^2, \end{aligned} \tag{2.36}$$

with trap frequencies

$$\omega_x = \sqrt{\frac{4U_0}{mw_x^2}}, \tag{2.37}$$

$$\omega_y = \sqrt{\frac{4U_0}{mw_y^2}}, \tag{2.38}$$

Property	Symbol	Value
Wavelength laser	λ	1070.6 nm
Laser frequency	ω_L	$2\pi \cdot 280$ THz
Resonance frequency ^{87}Rb	ω_0	$2\pi \cdot 384$ THz
Maximum laser power*	P	10.4 W
Beam waist x-direction*	w_x	23.5 μm
Beam waist y-direction*	w_y	41 μm
Rayleigh range	z_R	2.17 mm
Trap depth	U_0	-0.94 mK
Scattering rate	Γ_{sc}	7.5 Hz
Trap frequency x-direction	$\omega_x/2\pi$	2.4 kHz
Trap frequency y-direction	$\omega_y/2\pi$	4.1 kHz
Axial trap frequency	$\omega_z/2\pi$	31 Hz

Table 2.1: Table containing the characteristics of the ODT. The properties with an * are measured, while the other properties are calculated from the theory.

$$\omega_z = \sqrt{\frac{2U_0}{m}\left(\frac{1}{2z_{R_x}^2} + \frac{1}{2z_{R_y}^2}\right)} = \sqrt{\frac{2U_0}{mz_{R_{\text{ell}}}^2}}. \tag{2.39}$$

The Rayleigh range for this elliptical Gaussian beam and is

$$z_{R_{\text{ell}}} = \frac{z_{R_x} z_{R_y}}{\sqrt{1/2(z_{R_x}^2 + z_{R_y}^2)}}. \tag{2.40}$$

The trap depth follows from inserting Equation 2.35 into Equation 2.26. In the experiment the trapping laser has a wavelength of 1070.6 nm, and a power of 10.4 W. The beam waist at focus is 47 μm in the vertical direction by 82 μm in the horizontal direction. The trapping depth of the ODT is $U_0 = -0.94$ mK. The scattering rate follows from Equation 2.27 and is 7.5 Hz. With Equations 2.37, 2.38 and 2.39 the trapping frequencies are calculated to be $\omega_x = 2.4$ kHz, $\omega_y = 4.1$ kHz and $\omega_z = 31$ Hz. Table 2.1 summarizes the properties of the ODT. Figure 2.8 gives a graphical representation of the trap depth in the x- and z-direction.

If we want to increase the lifetime of the ODT, evaporative cooling can be used [18]. While evaporative cooling has not been used in the experiment yet, it can still be used in future experiments. To obtain evaporative cooling the intensity of the laser beam is reduced to decrease the trap depth. High energetic particles will escape from the trap. The remaining particles will thermalize through elastic collisions. The atom density in the trap is reduced, but the collision rate is also lower. The lifetime of the trap will thus be longer. The loss of atoms during the evaporative cooling can be high however. To reduce the high atom loss, we can implement a crossed-beam ODT. The crossed-beam ODT has also not been used in the experiments yet. If the temperature of the atoms

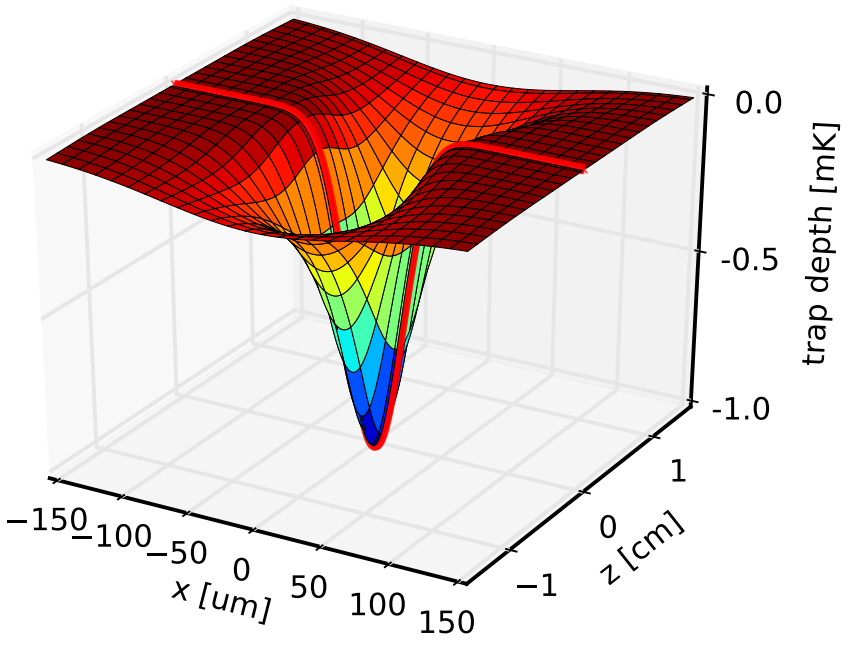

Figure 2.8: The trap depth in both x- and z-direction of a red detuned Gaussian ODT, with properties listed in Table 2.1.

turns out to be too high for the experiment, a combination of evaporative cooling and crossed-beam trapping can be used. Therefore the theory of the crossed-beam trap will be explained in the next section.

Crossed-beam trap optical dipole trap

A problem of the single beam ODT is the anisotropy of the trap, as the confinement is weak along the axial direction. A solution to get an isotropic atom cloud is to direct a second beam perpendicular to the first beam, crossing at the focus of the beams. This beam must have an orthogonal polarization to avoid interference effects [10]. The crossed-beam potential is a superposition of two single beam potentials. For two elliptical beams the potential then is

$$\begin{aligned} U_{\mathrm{cross}}(r,z) \simeq -U_1 \left(1 - \frac{2x^2}{w_{1x}^2} - \frac{2y^2}{w_{1y}^2} - \frac{1}{2}z^2\left(\frac{1}{z_{R_{1x}}^2} + \frac{1}{z_{R_{1y}}^2}\right)\right) \\ -U_2 \left(1 - \frac{2x^2}{w_{2x}^2} - \frac{2y^2}{w_{2y}^2} - \frac{1}{2}z^2\left(\frac{1}{z_{R_{2x}}^2} + \frac{1}{z_{R_{2y}}^2}\right)\right), \end{aligned} \tag{2.41}$$

where the subscripts 1 and 2 denote the two beams. The trapping frequencies following from the harmonic approximation are

$$\omega_{\mathrm{x,cross}} = \sqrt{\left(\frac{4U_1}{mw_{1x}^2} + \frac{4U_2}{mw_{2x}^2}\right)}, \tag{2.42}$$

$$\omega_{\mathrm{y,cross}} = \sqrt{\left(\frac{4U_1}{mw_{1y}^2} + \frac{2U_2}{mz_{R_{2,ell}}^2}\right)}, \tag{2.43}$$

$$\omega_{\mathrm{z,cross}} = \sqrt{\left(\frac{4U_2}{mw_{2z}^2} + \frac{2U_1}{mz_{R_{1,ell}}^2}\right)}. \tag{2.44}$$

The laser cooling in a crossed-beam trap leads to densities greatly exceeding those typically obtained in other optical dipole traps [19]. The atoms in the crossed-beam trap are localized to the overlapping volume of the two beams. The spatial density in this region is much higher. The geometry of the crossed-beam trap gives the trap a strong, nearly isotropic trap frequency.

CHAPTER 3

Experimental setup Magneto optical trap

In this chapter the experimental setup of the MOT is explained. In Section 3.1 the vacuum system in which the MOT operates is described. The details on the magnetic field and laser beams of the MOT are explained in Section 3.2 and 3.3. In the end we want to know the number of atoms that are trapped in the MOT. For this the fluorescence of the atoms that are trapped inside the MOT has been measured with a photodiode. Section 3.4 explains how we can obtain the number of atoms trapped inside the MOT from the fluorescence.

3.1 Vacuum chamber

The MOT traps the atoms inside a vacuum chamber. The low background pressure of the vacuum chamber ensures that collisions of atoms in the MOT with the background gas are minimized. Figure 3.1 gives an overview of the setup of the vacuum chambers. The atoms are first loaded into a 2-D MOT. Once the atoms are cooled by the 2-D MOT a push beam transports the atoms to the 3-D MOT chamber. The push beam is on resonance with the ^{87}Rb atoms. A differential pumping section between the 2-D MOT chamber and the 3-D MOT chamber maintains the pressure difference between the two chambers. The pumping section consists of a metal cylinder with a small hole. Only atoms travelling with a small solid angle along the direction perpendicular to the hole will travel through the pump section and reach the 3-D MOT. To maintain the vacuum in the chambers, ion getter-pumps are used, in combination with a titanium sublimation pump. The pumps lower the pressure to $\sim 10^{-7}$ mbar in the 2-D MOT chamber, and $\sim 10^{-10}$ mbar in the 3-MOT chamber.

The atom source is an ampul of 1 g metallic rubidium, with a natural abundance of 72.17% ^{85}Rb and 27.83% ^{87}Rb. The ampul is heated to a temperature between 60°C and 90°C. After the rubidium atoms are heated they are trapped by the 2-D MOT.

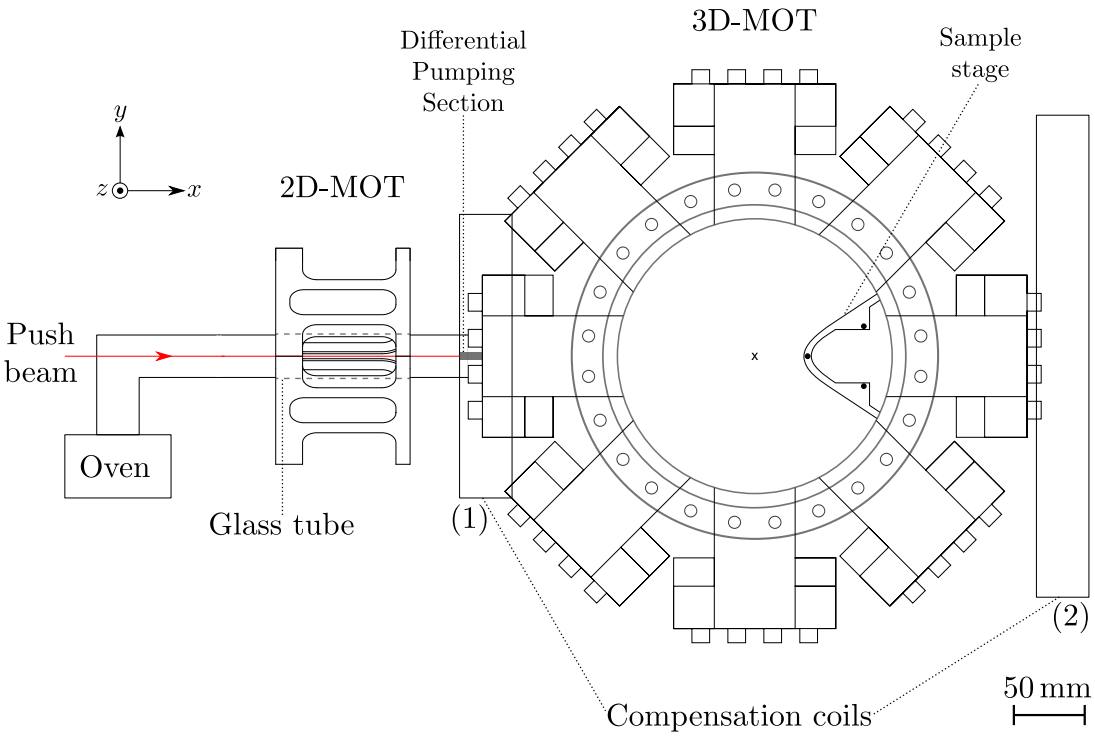

Figure 3.1: Schematic representation of the vacuum chambers setup [6].

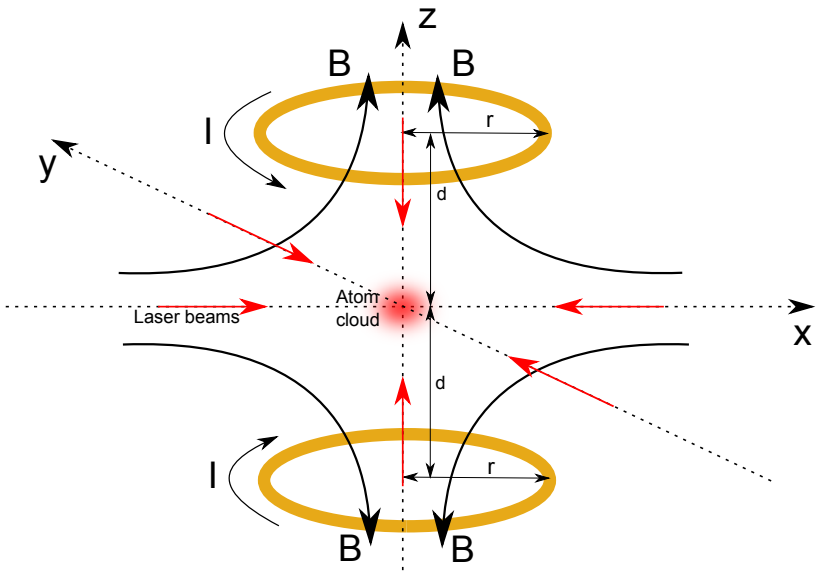

Figure 3.2: Magnetic field inside 3-D MOT in anti-Helmholtz configuration

3.2 Magnetic field

To create the position-dependent force on the atoms, a magnetic field gradient is required in both the 2-D MOT and the 3-D MOT. Three sets of coils are used to create the magnetic field gradients.

The 2-D MOT traps the atoms in two dimensions, while the atoms are free to move along the direction of the push beam. To create a 2-dimensional MOT a quadrupole magnetic field is formed. This is achieved by creating a setup of four rounded rectangular coils with 81 windings each centered around the 2-D MOT. A current of 2 A runs through the coils which are connected in series, creating a magnetic field gradient of 7.70 G/cm. There is no magnetic field along the unconfined x-axis. The atoms are trapped along this axis in a cigar-formed shape. The Ohmic resistance of the current through the coils causes heating. Therefore the coils are water cooled.

The 3-D magnetic field is created by two coils with 180 windings in anti-Helmholtz configuration. The setup of an anti-Helmholtz coil configuration is shown in Figure 3.2. The coils have a radius of 13.4 cm, and the center of the coils is located at a distance of 8.9 cm from the atom cloud. The coils are connected in series again with a current of 15 A going through the coils. A current of 15 A creates a magnetic field gradient of 16.01 G/cm. Water cooling is used again to cool the coils.

The magnetic field gradient created by the coils of the 3-D MOT disturbs the magnetic field of the 2-D MOT along the x-axis. This disturbance needs to be compensated for. Two compensation coils are used to correct the 2-D MOT magnetic field. These coils are placed in anti-Helmholtz configuration along the axis of the push beam. Compensation Coil 1 in Figure 3.1 has 320 windings and a diameter of 20 cm. It is placed at 17.5 cm from the center of the 3-D MOT. Compensation Coil 2 is put in place on the other side of the 3-D vacuum chamber. This coil is located at a distance of 21 cm from the center of the 3-D vacuum chamber. The diameter of this second compensation coil

is 27 cm, and the coil also has 320 windings. The compensation coils are also connected in series and carry a current of 2.3 A.

3.3 Diode lasers MOT

In the 2-D and 3-D MOT setup a total of 5 diode lasers are used. The diode lasers emit linearly polarized light at a central wavelength of 780 nm. The lasers are monitored by a temperature controller and a current controller.

The first diode laser is used as a reference beam for the offset locks of the cooling lasers. The offset locks are used to stabilize the lasers at the right frequency. Appendix B explains how the locking of the laser frequency works. The reference beam operates at the (1,3) crossover transition. Apart from being used as a reference beam, the first diode laser is also used as a push and probe beam. Two parts of the beam of the first diode laser are split off by beam splitter cubes, and shifted to resonance by AOMs. The first part, referred to as the push beam, pushes the atoms from the 2-D to the 3-D MOT. This increases the loading rate of the 3-D MOT. The second part, referred to as the probe beam, is used for absorption imaging. Absorption imaging is used to obtain the trapped atom number in the ODT, and is explained in Section 4.3.

For both the 2-D MOT and the 3-D MOT we need a laser to **cool** the atoms and a laser to **repump** the atoms as is described in Section 2.2. Parts of the laser beams are split off for spectroscopy. Spectroscopy is used to lock the lasers at the right transition frequency. Table 3.1 gives an overview of the transitions to which the lasers are locked.

For the 2-D MOT we need two pairs of counter-propagating beams with circular polarization, while for the 3-D MOT we need three pairs of counter-propagating beams with circular polarization. To change the polarization of the cooling and repump light from linear to circular polarization $\lambda/4$-waveplates are used. The cooling and repump beam are overlapped. Polarizing beams splitter cubes in combination with $\lambda/2$ waveplates split the 2-D MOT cooling/repump beam into 4 beams, and the 3-D MOT cooling/repump beam into 6 beams. The split beams have approximately equal power. The 2-D and 3-D MOT cooling/repump beams are then directed into respectively the 2-D and 3-D MOT vacuum, where they overlap in the centre where the magnetic field is zero. This is the position where the atoms are trapped.

3.4 Atom number measurement by fluorescence

To obtain the number of trapped atom in the MOT we measure the fluorescence of the atom cloud. The cloud of atoms is excited by a near resonant laser beam. By illuminating the atoms with near resonant light a maximum scattering rate is obtained. The scattering of the light is isotropic, which means that, if we can capture part of the scattered light, we know the total amount of light scattered by the atoms. Part of the scattered light is captured by a photodiode, which is a semiconductor device which converts light into a current or voltage. The scattering rate, and thus the amount of light captured by the photodiode, is dependent upon the amount of atoms in the atom

Laser	Locked	Detuned to lock
Reference	(1,3) Crossover	-
Push/Probe	(1,3) Crossover	212 MHz
2-D cooling	Reference	204 MHz
2-D repump	$F = 0 \rightarrow F^{'} = 2$	-
3-D cooling	Reference	193 MHz
3-D repump	$F = 0 \rightarrow F^{'} = 2$	-

Table 3.1: Table containing the transitions to which all the diode lasers of the MOT are locked. Some lasers are detuned to the lock by using an offset lock. Note that by locking the 2D cooling and 3D cooling laser with a detuning of respectively 204 MHz and 193 MHz to the (1,3) crossover transition, the 2D cooling and the 3D cooling lasers are locked respectively -8 MHz and -18 MHz to the cooling transition.

cloud. Therefore, we can obtain the number of atoms trapped in the MOT from the current or voltage measured by the photodiode. We can obtain the number of trapped atom in the MOT from the photodiode voltage in the following way. The number of photons Γ_{p} scattered by the atom cloud per second when light with a detuning Δ to the resonance frequency illuminates the atoms is

$$\Gamma_{\mathrm{p}} = \Gamma_{\mathrm{sc}} N_{\mathrm{a}}, \tag{3.1}$$

with Γ_{sc} the scattering rate of Equation 2.2, and N_{a} the number of atoms in the atom cloud. Only a fraction of these photons arrives at the photodiode. Because scattering is isotropic, this fraction is equal to the area of the photodiode divided by the area of a sphere with a radius equal to the distance between the atom cloud and the photodiode, $A_{\mathrm{PD}}/A_{\mathrm{Sphere}}$. The number of photons perceived by the photodiode per second is

$$\Gamma_{\mathrm{p,PD}} = N_{\Gamma p} \cdot \frac{A_{\mathrm{PD}}}{A_{\mathrm{Sphere}}}, \tag{3.2}$$

With $A_{\mathrm{Sphere}} = 0.26$ m^2, while $A_{\mathrm{PD}} = 5.1 \cdot 10^{-4}$ m^2. Each photon has an energy $E_p = \frac{hc}{\lambda} = 2.5 \cdot 10^{-17}$ J, with $\lambda = 780$ nm. The photons are converted into a current by the photodiode with a responsitivity $\eta = 0.52 \pm 0.02$ A/W. The current is directed through a resistor which converts the current into a voltage V with a gain of $\zeta = (2.38 \pm 0.05) \cdot 10^5$ V/A. The relation between the number of photons that arrive at the photodiode per second and the measured voltage is

$$\Gamma_{\mathrm{p}} = \frac{1}{\eta \zeta E_p} V, \tag{3.3}$$

By combining Equation 3.1, 3.2, and 3.3 we obtain the relation between the number of atoms trapped in the MOT and the measured voltage of the photodiode

$$N_a = \frac{A_{\mathrm{Sphere}}}{A_{\mathrm{PD}}} \frac{V}{\eta \zeta E_{\mathrm{p}} \Gamma_{\mathrm{sc}}} \tag{3.4}$$

Property	Symbol	Value
# atoms trapped in 3-D MOT	-	$4 \cdot 10^{10}$
Current 2-D MOT coil	I	2.0 A
Current 3-D MOT coil	I	15.0 A
Current compensation coil	I	1.8 A
Power push beam	P	230 μW
Total power 2-D cooling beam	P	193 mW
Total power 3-D cooling beam	P	74 mW
Detuning 2-D cooling laser	δ_{2D}	-18 MHz
Detuning 3-D cooling laser	δ_{3D}	-8 MHz

Table 3.2: Table containing the parameters of MOT atom measurement.

A measurement has been performed on the number of atoms trapped by the MOT. The detuning of the near resonant beam $\Delta = -18$ MHz, and the saturation parameter $s = 23.9$. A voltage of 2.9 V was measured, which gives us a total atom number of $N_a = (4.0 \pm 0.2) \cdot 10^{10}$ trapped in the MOT. Table 3.2 summarizes the relevant parameters during the MOT atom number measurement. The optimization of the parameters of the MOT has been performed by Verboven (2013) [20].

The above measurement was performed before doing the ODT measurements. The number of atoms trapped in the MOT is largely dependent upon the alignment of its lasers. Small changes in alignment can already create a large difference in the MOT atom number. Therefore the MOT atom number can change in between experiments. For measurements of the ODT atom number it is mainly important that the number of atoms trapped by the MOT during each measurement of an experiment is approximately constant. Therefore we have monitored the amount of atoms trapped by the 3-D MOT during the ODT experiments.

CHAPTER 4

Experimental setup optical dipole trap

In this Chapter the experimental setup of the optical dipole trap (ODT) is explained. The ODT loads the atoms from the MOT and transport them towards the sample. Section 4.1 gives an overview of the setup that has been built to achieve this. Section 4.2 is devoted to the effects of diffraction of the beam. Diffraction effects may be caused by reflections of the beam by, or transmissions through small sized objects. Diffraction can change the ODT depth and shape. This section shows the requirements of the optics to avoid diffraction effects. Eventually we want the ODT to load and transport as many atoms as possible. To observe the number of atoms trapped in the ODT a measurement method is needed. While for the MOT fluorescence of the atoms ($\sim 10^{10}$) was measured, the amount of atoms trapped in the ODT ($\sim 10^5 - 10^6$) is too low to easily measure with fluorescence imaging. The method used to measure the number of atoms in the ODT is absorption imaging. Section 4.3 explains how absorption imaging works, and explains how we can obtain the number of atoms in the ODT from absorption imaging. Finally in Section 4.4 the timing sequence of the full experiment is explained.

4.1 Overview experimental setup

The setup of the ODT consists of two layers on top of each other. These layers contain the optics of the experiment. We will start by explaining the optics of the bottom layer, followed by a desciption of the optics of the top layer.

The ODT is created by a 20 W continuous wave Ytterbium fiber laser with a wavelength of 1070.6 nm (IPG Photonics model YLR-20-LP). The laser outcoupler is located on the first level. The bottom layer has two functions. The optics of the bottom layer split the laser beam to make it possible to generate a crossed-beam ODT. The beam that is used for horizontal movement of the atoms will be referred to as the 'main beam'. The second beam which can be used to generate a crossed-beam ODT is referred to as

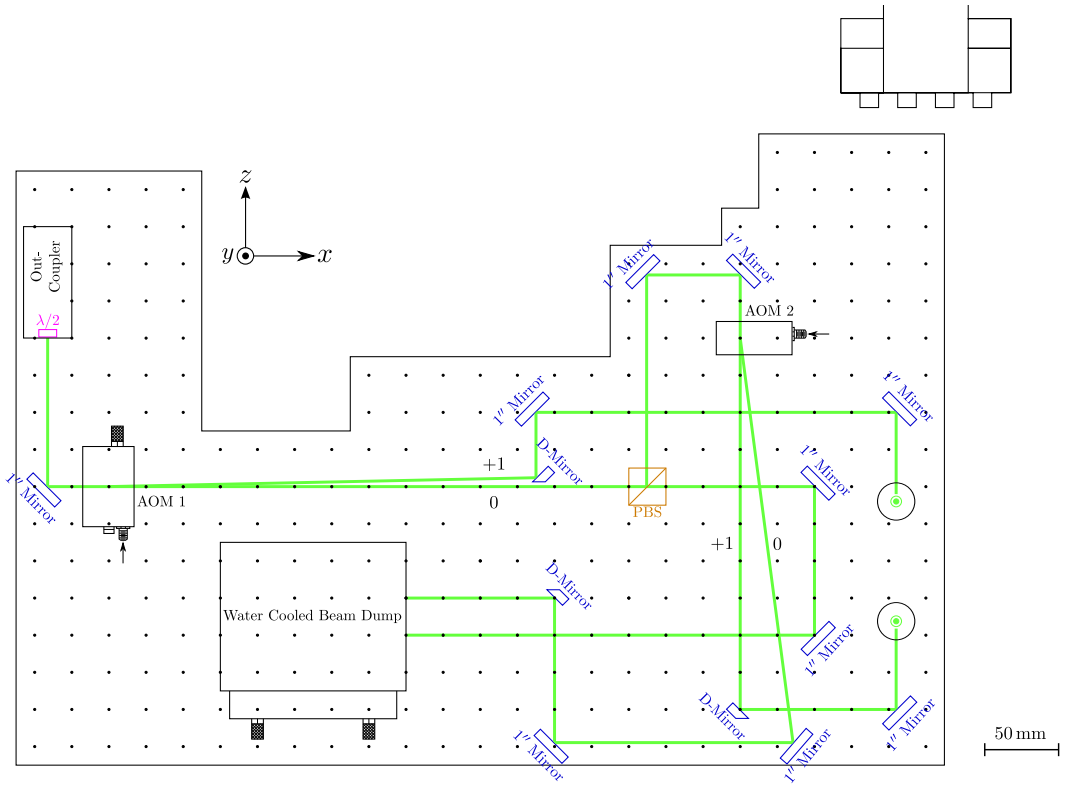

Figure 4.1: The bottom layer of the optical dipole trap setup. [6]

the 'cross beam'. Note that the crossed-beam is not used in our experiment. The second function of the bottom layer is to make the laser beam power controllable. In this way the trap depth can be controlled, in case evaporative cooling will be used in the future.

Figure 4.1 gives a schematic representation of the bottom layer of the ODT setup. The laser beam first goes through a high-power acousto-optical modulator (AOM, Isomet model M1135-T80L-3). The AOM (AOM 1) uses the acousto-optical effect to diffract the intensity and shift the frequency of light using sound-waves. In the AOM a crystal is attached to a piezo-electric transducer. An oscillating electric signal drives this transducer, such that the vibration creates acoustic waves in the crystal. These acoustic waves have maxima and minima, which locally change the index of refraction in the crystal. This change in index of refraction causes the incoming light to scatter. The incoming beam is refracted by an AOM into a number of beams with order n. By changing the frequency of the acoustic waves, the frequency of the diffracted laser beam can be controlled. The intensity of the laser beam can be controlled by changing the amplitude of the electric signal that drives the transducer. The diffraction efficiency indicates the percentage of the incoming beam that can be deflected into the first diffraction order. The diffraction efficiency of AOM 1 is approximately 94%. The separation angle created by the AOM between the 0th and 1st order is 21.0 mrad. The 1st order beam is the main beam, while the 0th order beam is the crossed-beam. Because the

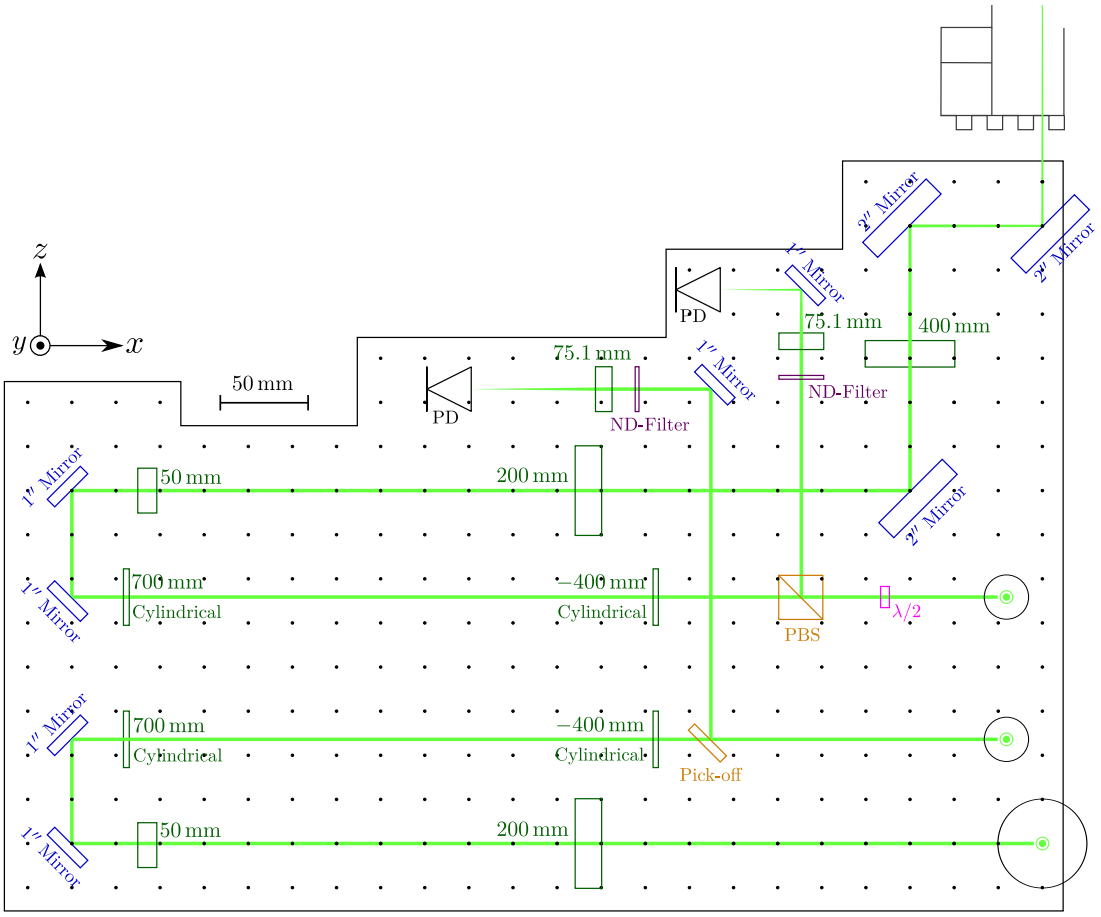

Figure 4.2: The top layer of the optical dipole trap setup [6]

AOM enables the power of both beams to be controlled, it is possible to use evaporative cooling on the atom cloud.

The zeroth order beam of AOM1 propagates through a beam splitter. The amount of light that is reflected and transmitted by the polarizing beam splitter cube (PBS) depends on the polarization of the light. The $\lambda/2$ waveplate positioned behind the outcoupler can control the polarization of the light and hereby the amount of light transmitted and reflected by the PBS. After being reflected by the PBS the cross beam is s-polarized light. Part of the cross beam that is transmitted by the PBS is directed into a water cooled beam dump. The beam that is reflected by the PBS is directed through a second AOM (AOM 2). Because the intensity of the cross beam is much lower than the intensity of the beam at the first AOM a different model AOM (AA Optic Electronic MTS80-A3-1064Ac) is used. This AOM separates the 1st diffraction order from the 0th diffraction order by 130 mrad, and has a deflection efficiency of about 90%. Note that the 0th order comes out under an angle, while the 1st order is not deflected by this AOM. The 0th order is directed to the beam dump, while the

1st order is used as the cross beam. Now the cross beam can be ramped with AOM 2 without changing the intensity of the main beam. The ramping of the intensity of the crossed-beam can be used for evaporative cooling.

The 1st diffraction order of AOM 1 and AOM 2 are both directed to the top layer. While being directed from the bottom to the top layer in the vertical path the beams both pass a pair of lenses. These pairs of lenses are used to collimate the beams, and compensate for the divergence of the beam coming out of the outcoupler.

At the top layer, part of the main beam is split by a PBS and directed onto a photodiode. A $\lambda/2$ waveplate is positioned in front of the PBS to determine the intensity of the transmitted and reflected beam again. The photodiode signal can be used as an error signal when controlling the power of the laser. Because the high intensity of the laser beam would saturate the photodiode, a neutral density (ND) filter is used to reduce the power of the beam. In a similar manner the error signal of the cross beam is obtained. The light that is transmitted by the PBS is p-polarized, such that the main beam is orthogonally polarized to the cross beam. The cross beam needs to be orthogonally polarized to the main beam in order for the intensity to exhibit no interference effects [10].

The transmitted part of both the main beam and the cross beam are directed through two telescopes. The shape and size of the beam waist at the focus determines the trap geometry. The shape of the beam waist is altered by the telescopes in such a way that in focus it overlaps well with the antinodes of the conveyor trap. The first telescope is a cylindrical telescope, which uses a set of a plano-concave and a plano-convex lens with a focal length of -400 mm and 700 mm. The separation distance between the lenses is 300 mm. This lens separation distance results in a magnification of 1.75 in the y-direction. The second telescope is a normal telescope which magnifies the beam waist in both directions equally. The normal telescope consists of a pair of achromatic doublets. The first achromatic doublet has a focal length of 50 mm, while the second achromatic doublet has a focal length of 200 mm. Located at a distance of 250 mm from each other, the lens combination magnifies the beam waist by a factor 4.

After going through the set of telescopes the main beam is directed towards the vacuum chamber, which contains the atoms trapped by the 3-D MOT. Before entering the vacuum chamber the beam is focused with a lens with a focal length of 400 mm. This lens is positioned such that the focus of the beam overlaps in the vacuum chamber with the location where the atoms are trapped by the MOT. The focus that is obtained with this lens has a beam waist of $w_{0,x} = 41$ μm in the x-direction, and $w_{0,y} = 23.5$ μm in the y-direction. The final mirror upon which the beam reflects before going into the vacuum chamber, is mounted on a rotating platform. This enables us to move the beam in the horizontal direction inside the vacuum chamber.

The cross beam after going through the two telescopes is directed to the top of the 3-D MOT vacuum chamber. From here it enters the vacuum chamber in the vertical direction. The focus of the cross beam must overlap with the focus of the main beam at the location we want to trap the atoms. The final part of the cross beam path, where

the beam is being directed into the vacuum chamber, is not implemented in the setup yet. The cross beam has not been used in the experiments.

4.2 Diffraction laser beam ODT

It is of main importance that the beam that eventually traps the atoms has a stable, Gaussian shaped beam focus. Diffraction of the beam can occur if the laser beam is reflected by or transmitted through an optical element with an aperture that is not much larger (or smaller) than the beam waist. Diffraction causes the intensity of the beam and the beam profile to be altered. Therefore it can change the trap depth and shape. The objective of this section is to analyse the beam propagation of a focused Gaussian beam clipped by an aperture. The waist of the ODT beam is largest after being magnified by the telescopes. Because the optical elements in the pathway of the beam after the first telescope all have a circular aperture, the analysis will be done with a circular aperture.

The trap depth is defined as the magnitude of the trapping potential at the focus of the trap. From Equation 2.26 we know that the trap depth is linearly proportional to the intensity at the focus. Therefore we want to determine the intensity at the focus, after the beam is diffracted by an aperture with radius r_a. In a paper of Gillen et al., (2010) [21] the on-axis intensity for a focused Gaussian beam clipped by a circular aperture is derived. In the derivation two assumptions are made. The location along the axis where we want to calculate the intensity $z >> \lambda$. Furthermore it is assumed that $z > r_a$. We want to derive the intensity at the focus which is located 26 cm from the last mirror upon which the laser beam reflects. As the aperture of this mirror is much smaller than 26 cm, both assumptions are correct. The on-axis intensity at focus is

$$I_{0,\text{diff}} = I_0(1 + \exp^{-2\gamma^2} - 2\exp^{-\gamma^2}), \tag{4.1}$$

with $I_{0,\text{diff}}$ the diffracted intensity at focus, I_0 the non-diffracted intensity at focus. The clipping ratio $\gamma = r_a/w_a$, with w_a the waist of the beam at the location of the aperture. If we plot Equation 4.1 against the clipping ratio we obtain Figure 4.3. For a clipping ratio $\gamma > 2.5$ more than 99% of the Intensity at the beam focus remains after reflection or transmission of the beam. From this we conclude that the size of the aperture of the optical elements needs to be at least 2.5 times the size of the beam waist. The beam waist after being magnified by the telescopes has a maximum size of $w_y = 7.7$ mm and $w_x = 4.4$ mm before being focused by the final lens. This means the radius of the aperture of the mirrors and lenses after the first telescope is preferably larger than 1.9 cm. Therefore we have chosen that all optical elements the beam passes through after going through the first telescope have a radius of aperture of at least 2 cm. Before the telescopes, the waist of the beam is approximately 2 mm. Therefore, the optical elements in front of the telescope have a radius of aperture of 1 cm or larger.

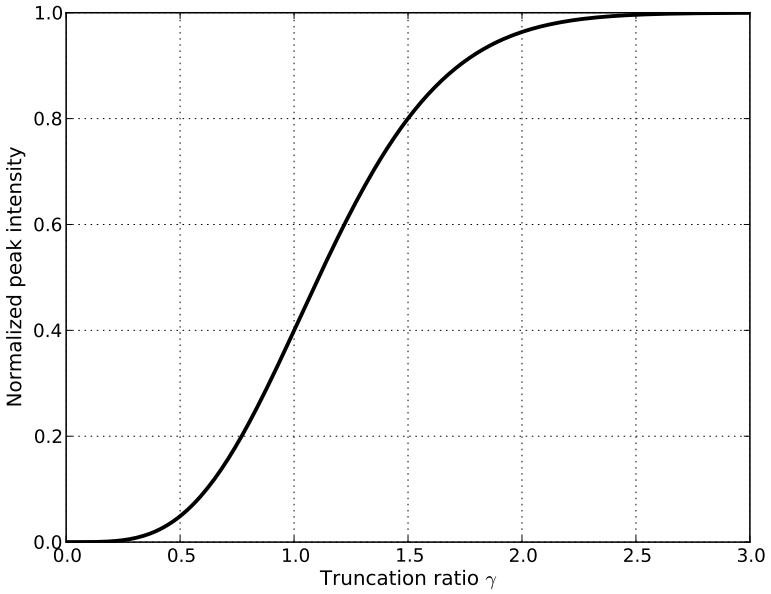

Figure 4.3: Normalized peak intensity in the focus of a Gaussian beam, after the beam has been diffracted by a circular aperture with clipping ratio γ.

4.3 Atom number measurement technique

To measure the atom number in the ODT absorption imaging is used. The absorption imaging technique works as follows. The 3-D MOT traps the rubidium atoms, such that in the middle of the vacuum chamber a big cloud of atoms forms. The dipole trap beam is overlapped with the rubidium cloud. Then both the beams and the coils of the 3-D MOT are switched off. The ODT has now trapped the atoms. To measure the amount of atoms in the trap, after a short period a probe beam is turned on at resonance with the atomic transition, while the ODT is turned off. The atoms will absorb part of the light that is on resonance. By measuring the intensity of the probe beam with a CCD camera (Andor iXon^3 885) located in the beam path behind the atom cloud, a reduction in intensity will be measured at the spot where the beam has passed through the atom cloud. To measure what part of the intensity reduction is caused due to the absorption of light by the atoms trapped in the ODT, a second shot is taken after the ODT is turned off and the atoms are not trapped anymore. After taking an image without atoms, the probe beam is turned off and a third dark image is taken. To obtain the transmittance of the beam going through the atom cloud, the following formula can be used

$$T = \frac{I_{\text{Atoms}} - I_{\text{Dark}}}{I_{\text{Flat}} - I_{\text{Dark}}}. \tag{4.2}$$

In Figure 4.4 an example is given of the different images the camera makes for absorption imaging. The camera images the atoms from a top view, perpendicular to the

propagation direction of ODT laser beam. In the "atoms" image the ODT is on, and we see a reduced intensity at the location where the atoms are trapped by the ODT laser beam. In the "Flat" image the ODT is turned off, and we do not see the atoms being trapped anymore.

The transmission T of the probe light after propagation through the cloud of atoms can also be described by Lambert-Beers law

$$T = \frac{I}{I_0} = \exp^{-OD} \tag{4.3}$$

with I_0 the intensity of the incoming laser beam, I the intensity of the transmitted laser beam, n the density of absorbed atoms, and OD the optical column density. The optical column density is

$$OD = n\sigma l, \tag{4.4}$$

with σ the rubidium absorption cross section, which is a measure for the probability of an absorption process, and l the distance travelled by the light through the atoms. The absorption cross section is [13]

$$\sigma = \frac{\sigma_0}{1+s}, \tag{4.5}$$

with $\sigma_0 = \frac{3\lambda^2}{2\pi} = 2.9 \cdot 10^{-13}$ m^2 the absorption cross section at resonance. The saturation intensity $I_{sat} = 3.6$ mW, while the probe beam intensity is $P = 148$ μW with a beam waist of $w = 7.4$ mm, giving us a $s = 0.05$. From Equation 4.3 we can derive that the OD is equal to

$$OD = -\ln(T) = -\ln\left(\frac{I_{\text{Atoms}} - I_{\text{Dark}}}{I_{\text{Flat}} - I_{\text{Dark}}}\right). \tag{4.6}$$

This means we can measure the OD. As $n = OD/\sigma$, and we can measure the OD we can calculate the number of atoms in the ODT. Measurements of the OD are performed in the following way.

To calculate the number of atoms a mask is made which covers the area at which the atoms are trapped. With Formula 4.6 the OD of each pixel beneath this mask is calculated. To subtract the noise from background atoms a mask is also placed on a location where the atoms are not trapped. The OD beneath this mask is then subtracted from the OD beneath the mask where the atoms are trapped. To determine the total number of atoms trapped by the ODT, the OD of each pixel is multiplied by the area of the pixel, and a summation is made over all the pixels beneath the mask. A lens has been used in the setup to focus the absorption image on the camera. After correcting for the magnification of the lens the total number of trapped atoms is

$$N_{\text{ODT}} = n \cdot V = n \cdot A \cdot l = \frac{A \cdot \sum_{\text{pix}} (OD_{\text{atoms}} - OD_{\text{background}})}{M\sigma} \tag{4.7}$$

$M = 0.85$ is the magnification factor and $A = 64$ μm^2 is the area each pixel. Before moving on to the experimental results, first the timing sequence of the experiment will be explained.

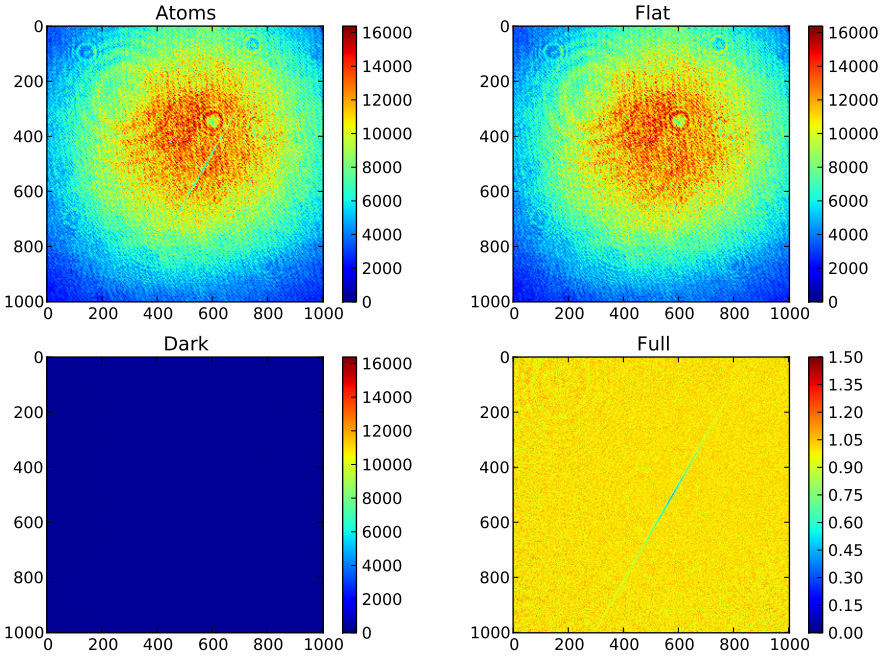

Figure 4.4: Absorption imaging of the atoms in the optical dipole trap. The x and y axis give the pixel count. The colour index in the atoms, flat, and dark image gives the photon count of a pixel. In the full image the colour index gives the transmission T.

4.4 Timing sequence experiment

The experiment is timed and controlled by an in house developed event generator based on a NXP LPC 1769 ARM CPU, hereafter referred to as the Puppet Master. A sequence code is written that can time actions by giving a trigger signal. This trigger signal can for example be "Turn the ODT beam on for 2 s", or "Give the camera an exposure trigger of 10 μs". With these signals a timing sequence can be generated.

In the experiment we use eight different channels, giving us eight controllable parameters. Figure 4.5 shows a typical timing scheme for an ODT atom number measurement. The measurement starts with loading the 3-D MOT. To load the 3-D MOT the 3-D coils, the cooling, repump and push beam are switched on. The time the 3-D coils are on is defined as the loading time. In the ODT experiments a loading time $t_{\text{load}} = 2.5$ s is used. To give the MOT time to stabilize before the MOT is turned off, the push beam is turned off before the magnets of the MOT are turned off. The 3-D MOT is now not loading anymore with high velocity atoms from the 2-D MOT and has time to stabilize. The time the MOT has to stabilize is $t_{\text{stabilize}} = 100$ ms. The magnets of the 3-D MOT are turned off 40 ms before the lasers fields are extinguished. This is advantageous because the resulting optical molasses cooling phase establishes the lowest possible temperatures and a quasi-thermal distribution in the trap [10]. The dipole trap beam is on while the 3-D MOT loads and stays on after the 3-D MOT has been turned off. The time that the optical dipole trap stays on after the coils of the 3-D MOT are turned off is called the holding time t_{hold}.

To obtain an ODT atom number from this experiment three images are taken, an image with atoms, an image without atoms, and a dark image, as is described in section 4.3. The first image with atoms is taken 2 μs after the ODT is turned off. This very short delay is to prevent the absorption frequency of the atoms to be shifted due to the ac Stark shift induced by the ODT beam [22]. To take the image with trapped atoms, the probe beam and the camera are turned on. After the atom image an image without trapped atoms is taken, by again turning on the probe beam and the camera after 60 ms. As the ODT has been turned off for 60 ms by now the atoms are not trapped anymore, and have had time to spread through the vacuum chamber. The final dark image is taken 60 ms after the image without atoms. For this image only the camera is turned on. The time the probe beam is turned on during the "atoms" and "flat" image is $t_{\text{probe}} = 100$ μs, while the time the camera is exposed to light is $t_{\text{exposure}} = 200$ μs. One measurement sequence takes between 5 and 15 s depending on the holding time of the ODT needed for the experiment. By varying t_{hold}, a lifetime measurement of the dipole trap can be done. The results of the lifetime measurement are presented in Section 5.2.

To optimize the loading of the atoms into the ODT, the frequency of the 3-D MOT cooling lasers is operated in two stages. First, the frequency detuning of the lasers is set close to resonance to optimize capture by resonant scattering forces. Once the MOT is loaded the frequency of its cooling lasers is changed to optimize sub-Doppler cooling, and to increase the atom number in the trap [23]. This process contains two time variables, the duration of the ramp t_{ramp}, and the time the ramp starts compared to

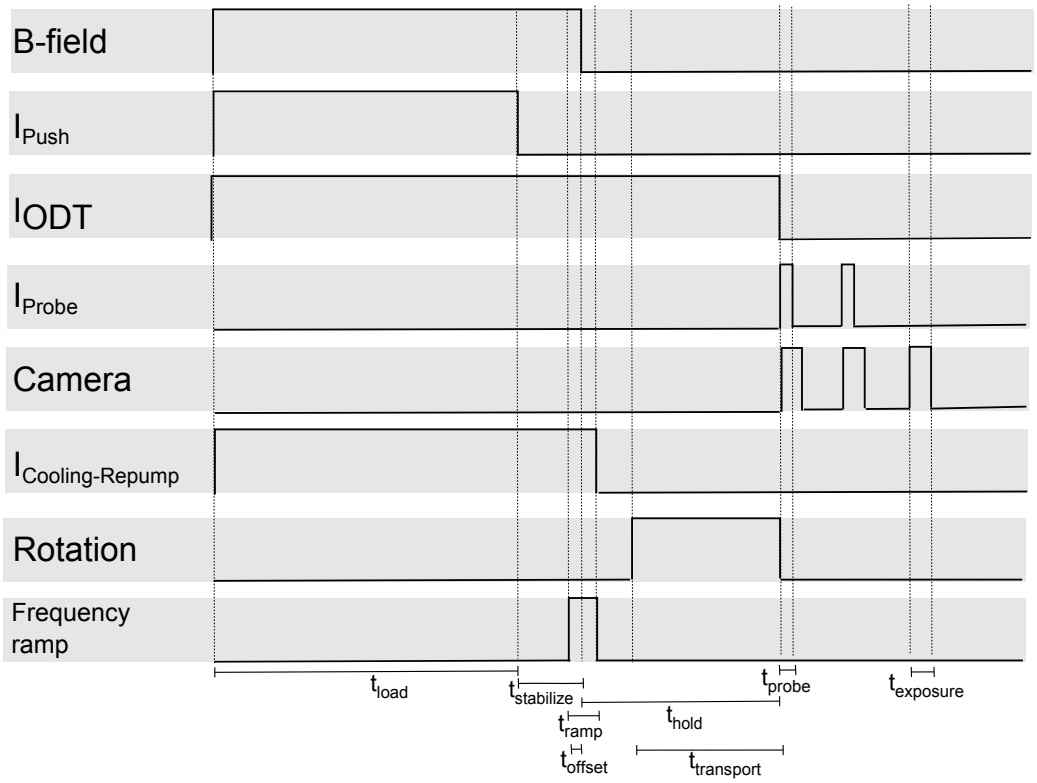

Figure 4.5: Timing sequence of a typical ODT atom measurement.

turning the magnets off t_{offset}. These two parameters, along with the frequency change during the ramping of the detuning have been optimized and the results are presented in Section 5.1.

In the final experiment we want to transport the atoms in the ODT. The time of transport is $t_{\text{transport}}$, and is optimized in Section 5.3.

CHAPTER 5

Results optical dipole trap

In this chapter the results of the atom number measurements of the ODT are presented and discussed. The experiments can be divided into three sections. The first experiment was performed to optimize the number of atoms loaded into the ODT. To increase the number of atoms loaded into the ODT the frequency detuning of the 3-D cooling lasers is ramped up just before the cooling lasers are turned off [24]. The results of this experiment are presented in Section 5.1. The second experiment measures the decay rate of the ODT. The ODT loses atoms due to collisions between two trapped atoms, and collisions of trapped atoms with the background gas. The lifetime results of the ODT can be found in Section 5.2. In the final experiment we transport the atoms from the location of the 3-D MOT towards the sample. Section 5.3 will discuss the atom losses in the ODT due to this transport. In this section we will also optimize the transport of atoms, by minimizing the transport losses.

5.1 Experiment 1: Loading of the optical dipole trap

Previous experiments have found that the number of atoms loaded into an ODT from a MOT can be increased by ramping up the detuned frequency of the MOT cooling lasers just before turning them off [24]. The physical process behind this is complex, and the real cause of the increase in loaded atoms is unknown. In Appendix B it is explained how we can achieve a ramp up the frequency of a laser beam.

The frequency ramp contains three variables. The first variable is the time in which the frequency is ramped t_{ramp}. The second variable is the frequency detuning from resonance up to which we ramp f_{ramp}. Before the frequency is ramped the frequency is detuned $\delta_{3\text{D}} = -18$ MHz to resonance of the cooling transition. The third variable is the timing of the ramp t_{offset}, compared to the turning off of the 3-D magnets. In three different experiments these variables are varied to optimize the number of atoms

Property	Symbol	Value
Current 2-D MOT coil	I	2.0 A
Current 3-D MOT coil	I	15.0 A
Current compensation coil	I	2.3 A
Power push beam	P	280 μW
Power probe beam	P	148 μW
Total power 2-D cooling beam	P	191 mW
Total power 3-D cooling beam	P	86.5 mW
Detuning 2-D cooling laser	δ_{2D}	-18.0 MHz
Detuning 3-D cooling laser	δ_{3D}	-8.0 MHz

Table 5.1: Table containing the parameters of MOT, during the ODT atom measurements.

loaded into the ODT. During these experiments the other parameters of the MOT are kept constant. Table 5.1 shows the MOT parameters during all ODT experiments. The ODT laser beam operates at 10.4 W. Each measurement is repeated five times, after which the average and standard deviation of each measurement are calculated.

5.1.1 Frequency ramp

The first experiment varies the frequency up to where we ramp f_{ramp}. The ramp ends at the time the coils of the 3-D MOT are turned off. The duration of the ramp is $t_{\text{ramp}} = 15$ ms. The atom number measurement is taken after the ODT has trapped the atoms for 150 ms. This is to make there are no remnants of the MOT, as the atoms trapped by the MOT have had time to fall by gravity and spread through the vacuum chamber. Figure 5.1 shows the amount of atoms trapped in the ODT after 150 ms for different f_{ramp}. If the frequency of the 3-D cooling lasers is not ramped approximately 162.000 atoms are caught in the trap after 150 ms. By ramping the frequency this amount can be increased to approximately 400.000 atoms. The ramping only increases the number of atoms in the trap up to a certain frequency. Ramping the detuning to more than -50 MHz has no significant effect on the amount of atoms loaded into the ODT anymore. Ramping the frequency to a detuning of more than -50 MHz does not significantly increase the amount of atoms loaded into the ODT anymore. For further experiments a ramped detuning of -78 MHz is chosen.

5.1.2 Duration ramp

The second experiment varies the duration of the ramp t_{ramp}. The ramp ends at the time the coils of the 3-D MOT are turned off. The measurements are again taken after a holding time of the optical dipole trap of 150 ms. The frequency of the 3-D MOT cooling laser is ramped from -18 MHz to -122 MHz from resonance. Figure 5.2 shows how the duration of the ramp influences the atom number trapped by the ODT. From this figure it follows that a very short ramp duration is favoured. The physical reason that a fast

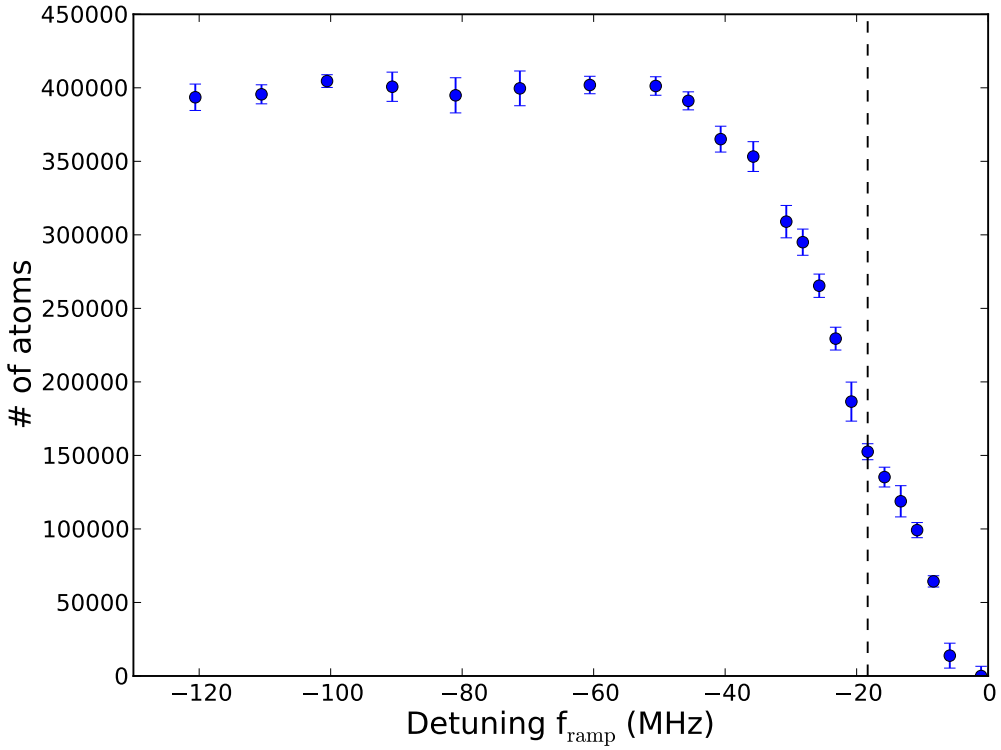

Figure 5.1: Number of atoms trapped in the ODT with $t_{hold} = 150$ ms, plotted against the detuning of the 3D MOT lasers after thr ramp of the laser frequency has been applied. The frequency of the laser beams of the 3-D MOT start with a detuning of -18 MHz to resonance indicated by the dashed line. The ramp that is applied changes the detuning up to frequency f_{ramp}. The duration of the ramp is 15 ms, and the ramp ends when the magnets of the 3-D MOT are turned off.

ramp is favoured is that by increasing the detuning also the trapping force working on the atoms decreases. If the frequency is ramped slowly, the atoms will therefore be lost from the trap. ramp duration of 15 ms is chosen for following experiments.

5.1.3 Offset ramp

The third experiment is performed to determine the timing of the frequency ramp. The timing of the start of the 15 ms ramp is varied with respect to the turning off of the coils of the 3-D MOT. The laser beams of the 3-D MOT are turned off approximately 40 ms after the magnets of the 3-D MOT. Figure 5.3 shows the results. The best time to change the detuning of the laser beams is 5 ms before turning the 3-D MOT magnets off. After the magnets are turned off there is no trapping mechanism anymore due to the lack of a magnetic field gradient, hence the ramp will not work. The ramp should not end before the magnets are turned off. The ramp increases the detuning. If this high detuning is maintained for a period the atoms will be lost from the trap because

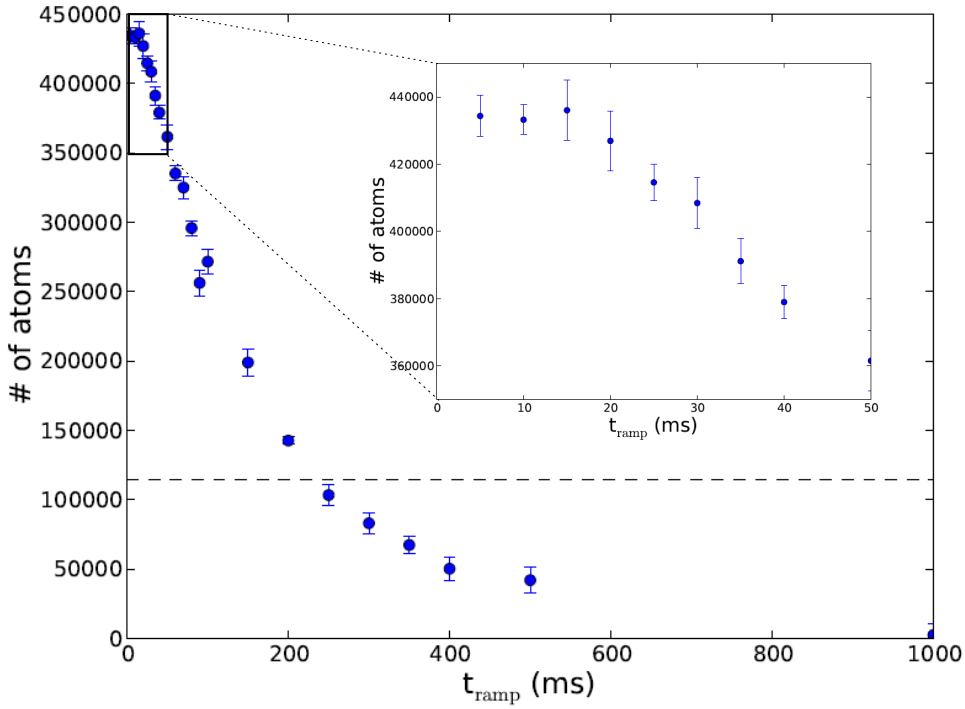

Figure 5.2: Number of atoms trapped in the ODT with $t_{hold} = 150$ ms for different ramp durations t_{ramp}. The ramp duration is the total time it takes for the frequency of the laser beam to be changed from the loading frequency of the cooling lasers of the 3D MOT to the ramped frequency of the lasers of the 3D MOT. The red detuning of the lasers of the 3D MOT is ramped from 18 MHz to 122 MHz. The ramp ends when the magnets of the 3-D MOT are turned off.

of the reduced trap force resulting from the high detuning. One would expect to get optimum loading for this 15 ms ramp starting 15 ms before the magnets are turned off. This is not the case as there is an internal delay of around 10 ms between shutting the current of the magnets and changing the frequency of the lasers. In future experiments the ramp will start 5 ms before the magnets are turned off.

5.1.4 Concluding remarks

Applying a fast increase in detuning of the cooling lasers of the 3-D MOT just before the ODT loads the atoms from the MOT increases the number of atoms loaded into the ODT. By ramping the detuning the atom number increases by a factor 2-3, from $\sim$ 160.000 atoms to $\sim$ 400.000. The detuning ramp is optimized and works best for $t_{\text{ramp}} = 15$ ms, $f_{\text{ramp}} > 50$ MHz red detuned to resonance, and $t_{\text{offset}} = -5$ ms compared to turning off the magnets of the 3-D MOT.

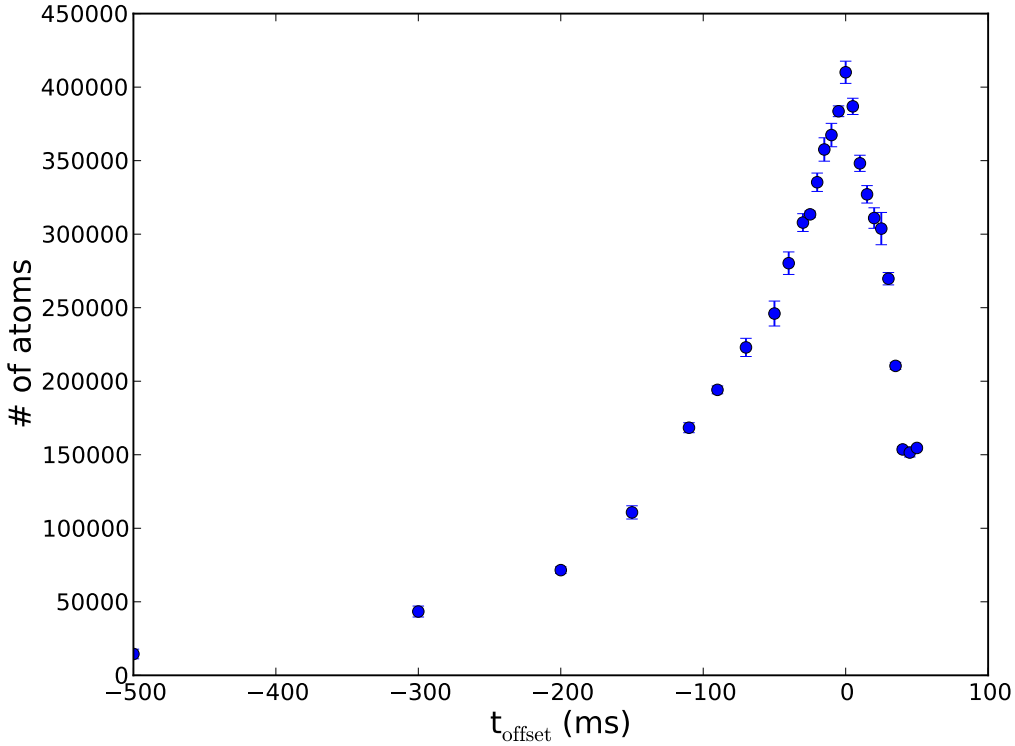

Figure 5.3: Number of atoms trapped in the ODT with $t_{\mathrm{hold}} = 150$ ms for different offsets of the start of the frequency ramp compared to the turning off of the 3D MOT magnets. The red detuning of the cooling lasers is ramped from 18 MHz to 122 MHz. The ramp duration is 15 ms.

5.2 Experiment 2: Decay rate in the optical dipole trap

The second experiment that has been performed measures the decay rate of the ODT. If no more atoms are loaded into the ODT the number of trapped atoms will decrease due to collisions with each other and the background gas. The measurement is performed by varying the holding time of the ODT, while keeping all other parameters constant. The result is the experimental decay curve of Figure 5.4.

A general model for trap loss in an optical trap is described by [25]

$$\frac{dN(t)}{dt} = -\alpha N(t) - \beta N^2(t), \tag{5.1}$$

where $N(t)$ is the number of atoms trapped in the ODT. The term with α includes losses due to collisions with the background gas, and losses due to the scattering of the dipole laser photons. The term with β contains the losses due to cold collision between trapped atoms or photoassociation. This equation can be solved and the solution is

$$N(t) = \frac{1}{A\exp(\alpha t) - B}. \tag{5.2}$$

In this solution $\beta = \alpha B$, and the number of atoms at $t = 0$ is $N_0 = 1/(A - B)$. With the least squares fitting method the parameters A, B, and α can be optimized to fit the experimental decay curve. This results in an $A = (2.7pm0.4)\cdot 10^{-5}$, $B = (2.5\pm0.4)\cdot 10^{-5}$, and $(\alpha = 2.0\pm0.2)\cdot 10^{-4}$ ms^{-1}. From this it follows that $(\beta = 4.9\pm0.9)\cdot 10^{-9}$ ms^{-1} and $N_0 = (5.8 \pm 1.1)\cdot 10^5$. By implementing these values in Equation 5.2, and plotting the equation, we find the fitted decay curve of Figure 5.4. The exponential lifetime τ_{ODT} of the ODT is defined as $1/\alpha$. With a laser power of 10.4 W, the exponential lifetime $\tau_{\mathrm{ODT}} = 5.1 \pm 0.6$ s.

To see how both the collisions of the atoms with the background gas (α-term), and collisions of the particles with each other (β-term) influence the loss, the contributions of both these terms to the total atom loss are plotted in Figure 5.4. The first 3.2 seconds the loss is mainly due to collisions of trapped particles with each other. After 3.2 seconds the trap density has decreased to such a value that the most atoms are lost due to collisions with the background gas.

To see how good the fit describes the data we use a reduced Chi-squared statistical analysis. This statistical analysis takes into account the variance of the measured data points σ^2 and the difference between observed value O and the model fit expected value E. The reduced chi-squared value is

$$\chi^2 = \frac{1}{\nu}\sum\frac{(O-E)^2}{\sigma^2}. \tag{5.3}$$

In this equation $\nu = N - n - 1$ is the number of degrees of freedom, with N the number of observations, and n the number of fitted parameters, assuming that the mean value is also a fitted parameter. If the match between observation and estimates is best in accordance with the error variance than the $\chi^2 = 1$. A $\chi^2 > 1$ indicates that the fit does not fully capture the data. A $\chi^2 < 1$ indicates that the model is over-fitting the

data. $\chi^2 = 0.63$ for the fit that we obtained, which is close to 1. This means that the fit and observations match well within the error variance.

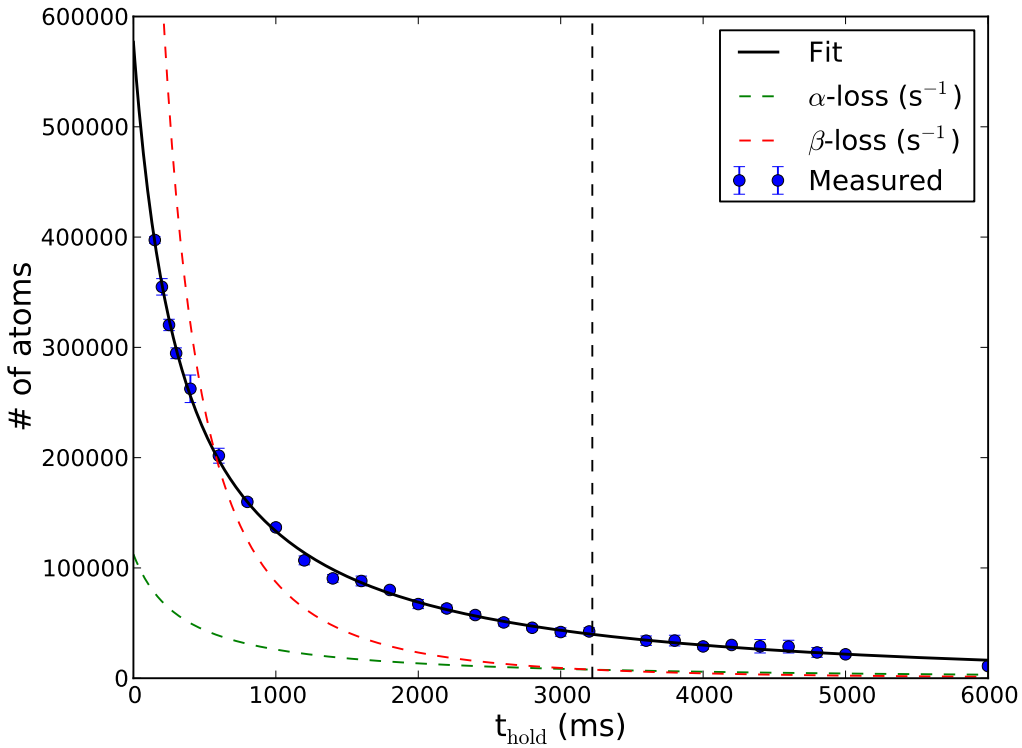

Figure 5.4: Decay measurement of the ODT. The number of atoms trapped in the ODT is plotted against the holding time of the trap. A fit to the measurements is made (black line). The ODT loses atoms due to collisions with the background gas (α-loss) and due to collisions of trapped atoms with each other (β-loss). After 3.2 seconds losses from collisions with other atoms and losses from collisions with the background are equally important, indicated by the dashed line.

5.3 Experiment 3: Transport of rubidium atoms with an optical dipole trap

The final step in the ODT experiment is to transport the atoms from the location of the 3-D MOT to the location of the sample where an optical conveyor trap will take over. To transport the atoms in a straight line, the focus of the dipole trap needs to move in a straight line. This is achieved by using a rotating mirror with an off-centre rotation axis as is schematically represented in Figure 5.5. The total distance that the atoms need to be transported is approximately 5 cm. This needs to be done in the most efficient way, losing the least amount of atoms. The atoms are transported by linearly accelerating the rotation of the mirror till the atoms are transported half-way. With the same linear deceleration the rotating mirror is slowed down until the final point is reached. The atom loss during the transport is dependent upon two parameters, the acceleration/deceleration of the atom cloud, and the time it takes to before the atoms are positioned at the sample. These parameters are entangled in a way that a faster acceleration and deceleration lead to a shorter transport time. More atoms are lost per second from the trap when accelerating faster, but the time it takes to reach the sample is shorter. This means there is a trade-off between having a gentle acceleration and taking the least time to reach the target. For convenience we will call the total atom loss in a measurement where we do not move the trap N^n_{loss}. If we do a measurement where the atoms are moved, the **extra** atom loss that results from transporting the atoms is called N^t_{loss}. The total atom loss in a moving ODT is N_{loss}=N^n_{loss}+N^t_{loss}. The goal of this section is to find the most efficient motion of the rotating mirror, thus we want to minimize N_{loss}.

As the imaging axis is located at the centre of the 3-D MOT vacuum chamber, to do measurements on the efficiency of transport the atoms have to be transported back and forth. The disadvantage of moving back and forth is that the atoms need to be accelerated and decelerated twice, resulting in a higher atom loss. However this does mean that the atom loss can only be smaller in the case where the atoms are moved towards the sample and only accelerated and decelerated once. Figure 5.6 shows the transport of the atoms, by imaging at different times during the transport process. Note that in this image only a small movement of the atoms is made to keep the atoms within reach of the imaging axis.

To optimize the acceleration and deceleration of transport of the atom cloud in the ODT the following experiment has been done. The mirror starts rotating 175 ms after the magnets of the MOT are turned off. In this experiment we will label the time from the turning off of the 3-D magnets until the mirror starts rotating t_{static}. The mirror rotates 5°, of which the first 2.5° it linearly accelerates and the last 2.5° it linearly decelerates. The acceleration and deceleration are equal in magnitude. The maximum acceleration that is used is 2000 $^\circ/\text{s}^2$ as faster accelerations are not possible. When the mirror reaches the final position it moves back immediately towards the original position in a similar fashion. The mirror will thus rotate 10° in total. The total time it takes for the mirror to rotate back and forth is called $t_{\text{transport}}$. As the focus of the trap is 26 cm

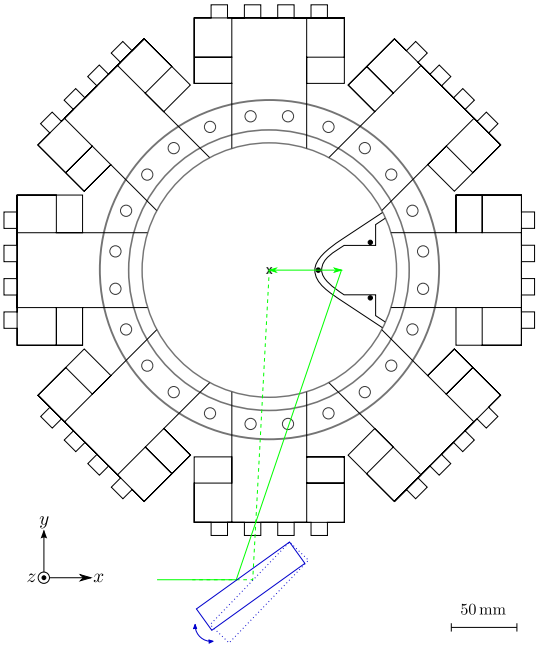

Figure 5.5: Schematic representation of the rotating mirror. Due to the off-centre rotation of the mirror the ODT beam focus which traps the atoms moves from the location of the 3-D MOT to the sample in a straight line.

away from the mirror, the focus of the trap moves approximately 9 cm in total. After the focus of the trap is back at the original position, immediately the number of atoms is measured by absorption spectroscopy. In this experiment $t_{\text{hold}} = t_{\text{static}} + t_{\text{transport}}$.

The number of atoms trapped in the ODT after the transport can be plotted as a function of acceleration/deceleration (Figure 5.7) and as a function of holding time (Figure 5.8). From these graphs it follows that it is favorable to move the atoms with a fast acceleration in a short time. Losses due to fast acceleration are less than losses due to a long holding time. Between 500 $^\circ/s^2$ acceleration ($t_{\text{hold}} = 560$ ms) and 2000 $^\circ/s^2$ acceleration ($t_{\text{hold}} = 360$ ms), the effects of losses due to a faster acceleration are compensated by a shorter holding time. This results in a plateau between 500 $^\circ/s^2$ and 2000 $^\circ/s^2$ acceleration.

The atom loss in an ODT where we do not move the trap, N^n_{loss}, is known from Figure 5.4. It can also be measured, what the extra losses are due to transporting the atoms, N^t_{loss}. To measure the extra transport losses we take a constant total holding time and vary the acceleration of transport. Instead of taking the atom number measurement after $t_{\text{hold}} = t_{\text{static}} + t_{\text{transport}}$, we take the measurement after $t^*_{\text{hold}} = t_{\text{static}} + t_{\text{transport}} + t_{\text{pad}}$. The padding time t_{pad}, is the time between which the rotation movement is finished and the measurement is taken, and is adjusted so that $t^*_{\text{hold}} = 600$ ms for all measurements. This is the time it takes for the slowest movement (acceleration of $400^\circ/s^2$) to be back just in time before the measurement is taken. A reference

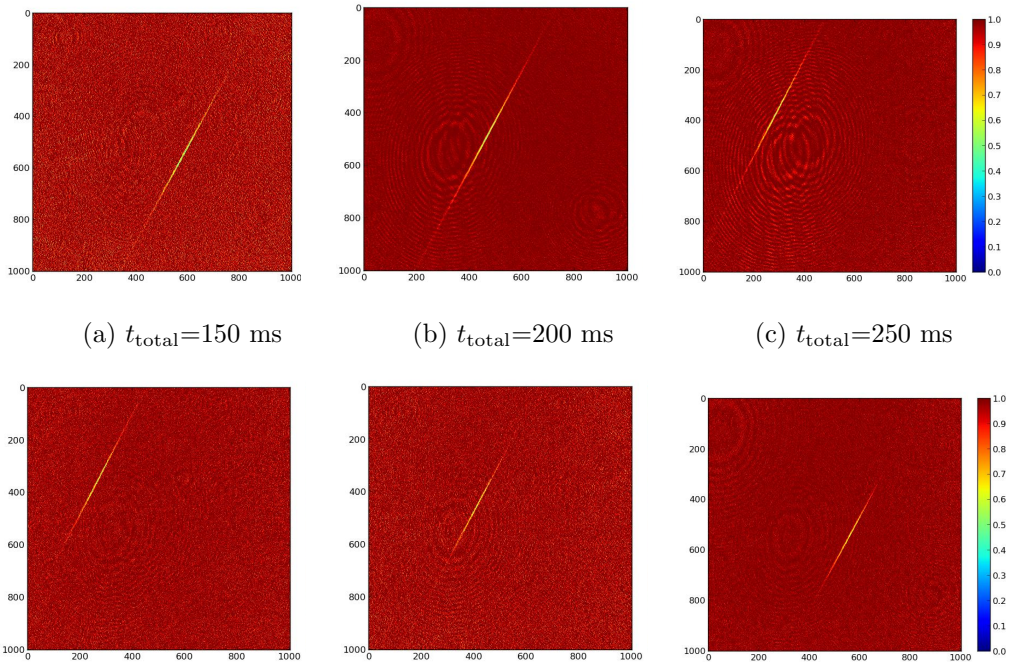

(a) t_{total}=150 ms (b) t_{total}=200 ms (c) t_{total}=250 ms

(d) t_{total}=300 ms (e) t_{total}=350 ms (f) t_{total}=400 ms

Figure 5.6: Absorption imaging of transport of rubidium atoms. The color index gives the transmission of the probe light. Absorption resulting from trapped atoms in the ODT can clearly be seen. The image is taken at different total holding times. The mirror rotates back and forth transporting the atoms as can be seen from the absorption image.

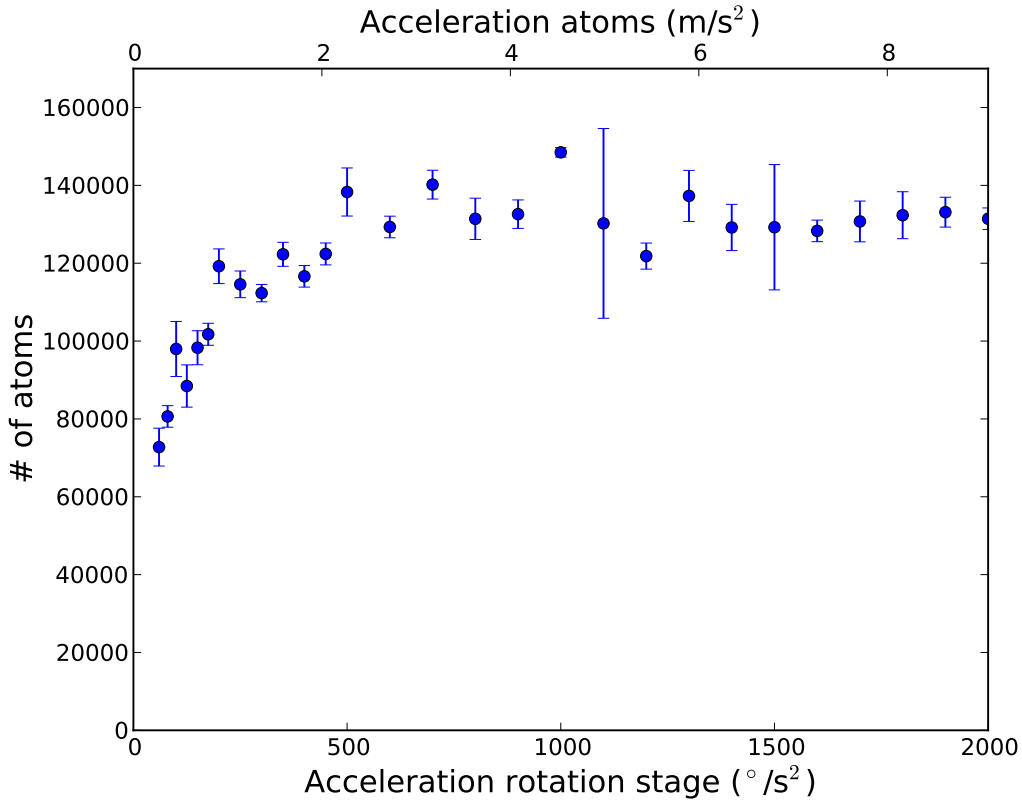

Figure 5.7: The number of atoms trapped in the ODT for different accelerations. The mirror rotates 5° towards the sample and 5° back to the initial position. The measurement is taken at the moment the atoms are back at the initial place.

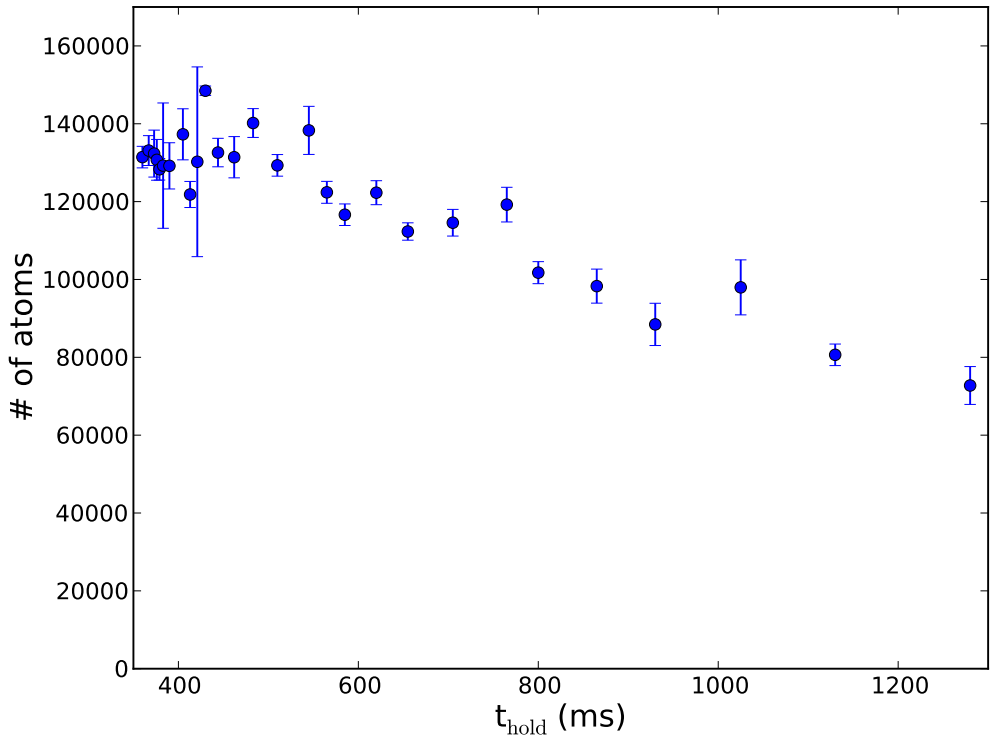

Figure 5.8: The number of atoms trapped in the ODT for different holding times. The mirror rotates 5° towards the sample and 5° back to the initial position. The image is taken at the moment the atoms are back at the initial place. This Figure contains the same data as Figure 5.7 but plotted against the holding time.

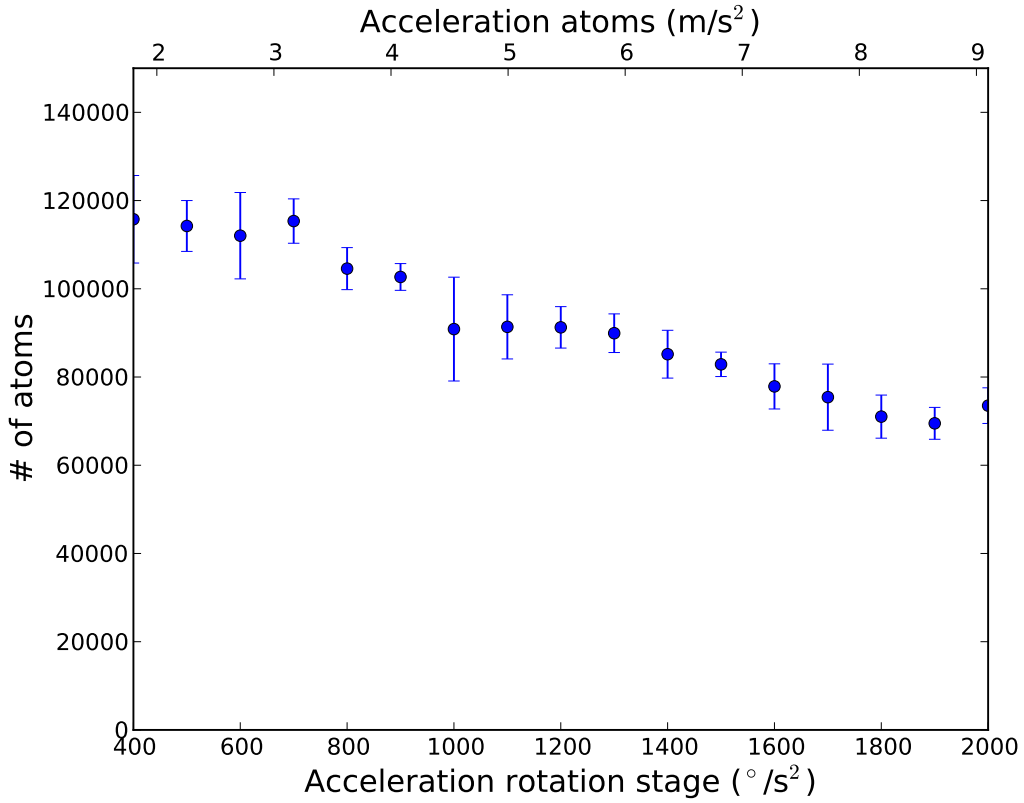

Figure 5.9: The number of atoms trapped in the ODT for different accelerations. The holding time is kept constant at t_{hold} =600 ms.

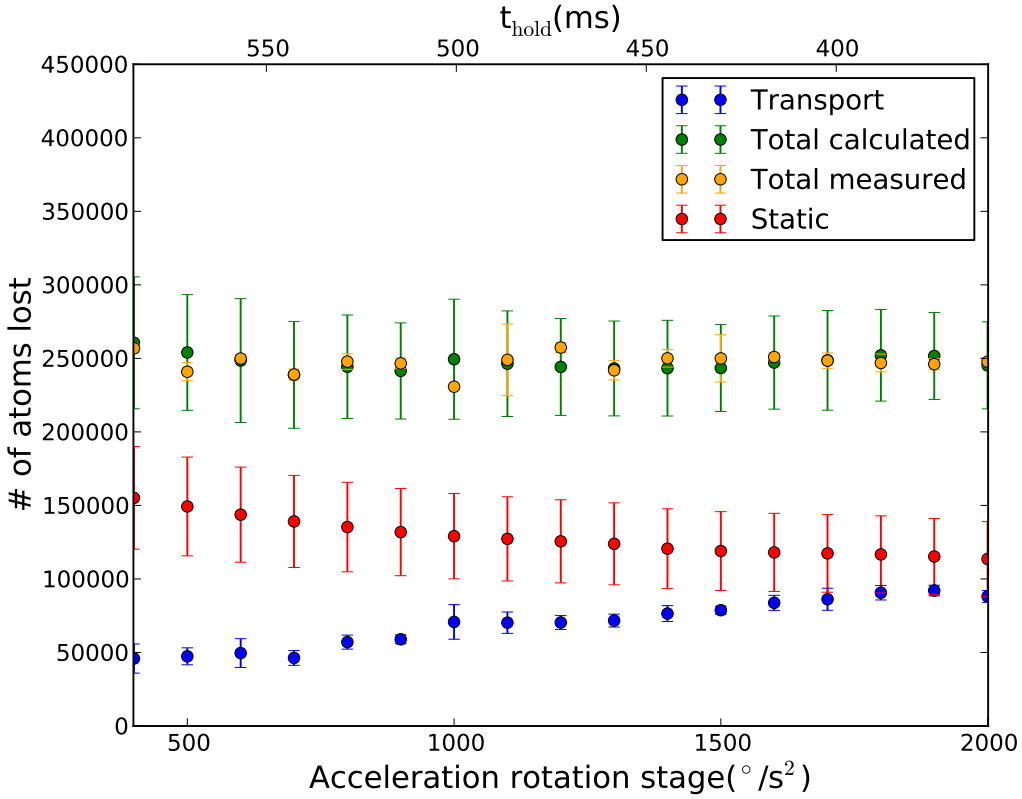

Figure 5.10: Number of atoms lost by the different mechanisms between $t_{\text{hold}} = t_{\text{static}}$ and $t_{\text{hold}} = t_{\text{static}} + t_{\text{transport}}$. For the static measurement the atom loss is measured during the same time period although no transport takes place.

measurement is taken without transport of the atoms, trapping 161.522 ± 8010 atoms after $t_{\text{hold}} = 600$ ms. The atom number in the ODT for different accelerations is shown in Figure 5.9. The loss due to transport $N^t_{\text{loss}} = N_{n,600\text{ms}} - N_{t,600\text{ms}}$, where $N_{0,600\text{ms}}$ is the number of atoms in a non-moving trap after 600 ms and $N_{t,600\text{ms}}$ is the number of atoms in the moving trap after 600 ms. Figure 5.10 shows the atom losses in the ODT from transport and from exponential decay without transport between $t_{\text{hold}} = t_{\text{static}}$ ms and $t_{\text{hold}} = t_{\text{static}} + t_{\text{transport}}$. We have measured the atom loss from transport (Figure 5.9) and the atom loss without the transport of the atoms separately (Figure 5.4). The exponential decay losses without transport are plotted against the holding time in Figure 5.10. If we add the two losses we obtain the calculated total atom loss. The calculated total atom loss can be compared to the measured total atom loss (from Figure 5.7 and Figure 5.8). The differences between the calculated total atom loss and the measured total atom loss are small. A note needs to be made that these losses strictly spoken can not be added linearly as transport causes heating, and the trap loses atoms during the transport. The graph of the different loss mechanisms does give an indication why there is a plateau between $400°/s^2$ and $2000°/s^2$.

To conclude an acceleration of the rotating mirror between 500 $^\circ/s^2$ and 2000 $^\circ/s^2$ gives the lowest atom loss during transport. The total number of atoms in the trap before transport is $\sim$ 400.000, while the total number of atoms after transport is $\sim$ 130.000.

CHAPTER 6

Conclusions

An optical dipole trap (ODT) has been build that can load ^{87}Rb atoms from a 3D-MOT and transport them towards a sample. For the ODT an Ytterbium fiber laser with a wavelength of 1070 nm is used to trap the atoms. The beam waist at focus is 47 μm in the vertical direction by 82 μm in the horizontal direction. An intensity of 10.4 W was used in the experiments. This results in a trapping depth of $U_0 = -0.94$ mK, and a scattering rate of 7.5 Hz. With the ODT three experiments have been performed.

The first experiment has been performed to increase and optimize the number of atoms loaded from the MOT into the ODT. A fast change in detuning of the cooling lasers of the 3-D MOT, just before the ODT loads the atoms from the MOT, increases the number of atoms trapped it the ODT. By ramping the frequency detuning the atom number loaded into the ODT increases from $\sim$ 170.000 atoms to $\sim$ 400.000 after a holding time of $t_{\text{hold}} = 150$ ms. The ramp is optimized and works best for a duration of the ramp $t_{\text{ramp}} = 15$ ms, a change in frequency of $f_{\text{ramp}} >$50 MHz, and a start of the ramp $t_{\text{offset}} = 5$ ms before the magnets of the 3-D MOT are turned off.

The second experiment was performed to measure the lifetime of the ODT. Due to collisions with the background gas (α-losses) and with other atoms(β-losses), the ODT loses atoms. A fit has been made to the decay of the atoms. The losses can be described by $\frac{dN(t)}{dt} = -\alpha N(t) - \beta N^2(t)$, with $(\alpha = 2.0 \pm 0.2) \cdot 10^{-4}$ ms^{-1}, $(\beta = 4.9 \pm 0.9) \cdot 10^{-9}$ ms^{-1}, and $N_0 = (5.8 \pm 1.1) \cdot 10^5$. With a laser power of 10.4 W, the exponential lifetime is $\tau_{\text{ODT}} = 5.1 \pm 0.6$ s.

The third experiment optimized transport of the the atoms from the MOT towards the sample. Atoms are lost from the ODT during transport, both due to acceleration of the atom cloud, and due to collisional decay. Faster transport will decrease atom loss due to collisional decay due to the shorter transport time, but will increase losses caused by a faster acceleration. There is a trade-off between these two losses. Between 500 $^\circ/s^2$ acceleration (t_{total}= 560 ms) and 2000 $^\circ/s^2$ acceleration (t_{total}= 360 ms) of the

rotation stage, the losses due to both mechanisms are at a minimum. The total number of atoms in the trap before transport is $\sim$ 400.000, while the total number of atoms after transport is $\sim$ 130.000. The total atom loss will be less in the final experiment, because in the transport measurements the atoms were moved to the sample and back to the location of the 3-D MOT in order to be able to image and measure the atom number. In the final experiment the atoms only have to be moved to the sample.

CHAPTER 7

Outlook

An optical dipole trap (ODT) which can transport atoms from the magneto-optical trap (MOT) to the optical conveyor has been build. The next step is to build an optical conveyor trap, of which the fundamentals are described in the master thesis of S. Greveling, and Z. Kluit [6, 7]. However there are still methods to improve the trap depth and atom number trapped by the ODT. This outlook will focus these methods.

A possible method to increase the number of atoms loaded into the ODT is to increase the density of the MOT. The density of the MOT can be increased by increasing the magnetic field gradient of the MOT before loading the atoms into the ODT. This can be achieved by ramping the current of the 3-D coils. It is important that the MOT cooling beams and ODT beam are aligned at the spot where the magnetic field is 0, as this is the location where the density increases most. A system of ramping the magnets has already been implemented in the setup. In the near future these experiments can be performed.

To increase the cooling of the atoms, and hereby increase the lifetime of the trap evaporative cooling can be used. Evaporative cooling can be achieved by reducing the intensity of the ODT beam, hereby decreasing the trap depth. The highly energetic particles will escape the trap. The remaining particles thermalize at a lower temperature. The setup has the possibility to ramp the intensity of the ODT beam due to the acousto-optical modulators (AOM's). A disadvantage of evaporative cooling is the high atom loss during the process. To obtain a higher atom number in the trap the crossed-beam trap can be implemented. The crossed-beam trap increases the atom density. [26].

Another method to increase cooling of the atoms is by ramping down the repump laser intensity of the 3-D MOT, just before turning the repump laser off. The repump laser ensures atoms do not get lost in the $F = 1$ ground transition, but also heats the atoms. By ramping down the intensity of this laser the heating is reduced. An AOM

could be used to ramp the repump intensity.

There is also a method to improve the efficiency of transport of the atoms by the ODT. Up till now the ODT accelerates and decelerates linearly. Due to an abrupt change in acceleration the atoms are heated. At the start of the transportation process the acceleration is instantly switched from 0 to a. After the atoms have been transported half the of the distance between the starting point and sample the acceleration changes from a to $-a$. This abrupt change in acceleration can be avoided by changing the jerk instead of the acceleration. The jerk is the derivative of the acceleration. If the jerk is switched from 0 to j the acceleration will gradually increase. A more gradual change in acceleration can reduce the atom loss.

Practice will show if these methods are necessary to be implemented or if the current number of atoms and temperature of the atoms prove to be sufficient for the final experiment.

APPENDIX A

Rubidium 87 transition hyperfine structue

Rubidium is an element of the alkali metal group with atomic number 37. The rubidium used in the experiments is ^{87}Rb, which is a radioactive element but has a half-life time of $4.88 \cdot 10^{10}$ year making it effectively stable. ^{87}Rb has two transitions that are components of a fine structure doublet, namely the $5^2S_{1/2} \rightarrow 5^2P_{3/2}$ and the $5^2S_{1/2} \rightarrow 5^2P_{1/2}$ transitions, which will be called the $D2$ and $D1$ line respectively. Both of these transitions also have a hyperfine structure.

The fine structure, which describes splitting of the spectral lines of atoms due to first order relativistic corrections, results from coupling of orbital angular momentum $\mathbf{L}$ of the outer electron and the spin angular momentum $\mathbf{S}$. The total angular momentum is:

$$\mathbf{J} = \mathbf{L} + \mathbf{S} \quad with \mid \mathbf{L} - \mathbf{S} \mid \leq \mathbf{J} \leq \mathbf{L} + \mathbf{S} \tag{A.1}$$

For the ground state of ^{87}Rb, $L = 0, S = 1/2$ and $J = 1/2$, while for the first excited state $L = 1$ so J is either $1/2$ or $3/2$. The energy transition from $L = 0$ to $L = 1$ is called the D line transition and is thus split into two components, where in the excited state $J = 1/2$ (D^1 or $5^2S_{1/2} \rightarrow 5^2P_{1/2}$) $J = 3/2$ (D^2 or $5^2S_{1/2} \rightarrow 5^2P_{3/2}$. The energy level labels contain the principal quantum number ($n = 5$), the superscript is $2S + 1$ and the subscript is the value of J.

Apart from the fine structure, to trap the atoms with a MOT also a hyperfine structure is needed. Hyperfine splitting is the splitting and shifting of energy levels of the atoms due to interactions of the nucleus with internally generated electric and magnetic fields. The splitting of the atomic energy levels is due to a different total atomic angular momentum $\mathbf{F}$, which is the result of the coupling of the total electron angular momentum $\mathbf{J}$ with the total nuclear angular momentum $\mathbf{I}$:

$$\mathbf{F} = \mathbf{J} + \mathbf{I} \quad \text{with} \mid \mathbf{J} - \mathbf{I} \mid \leq \mathbf{F} \leq \mathbf{J} + \mathbf{I} \tag{A.2}$$

For the ground state of ^{87}Rb $J = 1/2$ and $I = 3/2$ so $F = 1$ or $F = 2$. The excited states are split into respectively four hyperfine states (for the D_2 line) with $F = 0, 1, 2, 3$ or two hyperfine states (for the D_1 line) with $F = 1, 2$. Figure A.1 and A.2 show the splitting of the energy levels due to the finestructure and hyperfine structure, along with their frequency shifts.

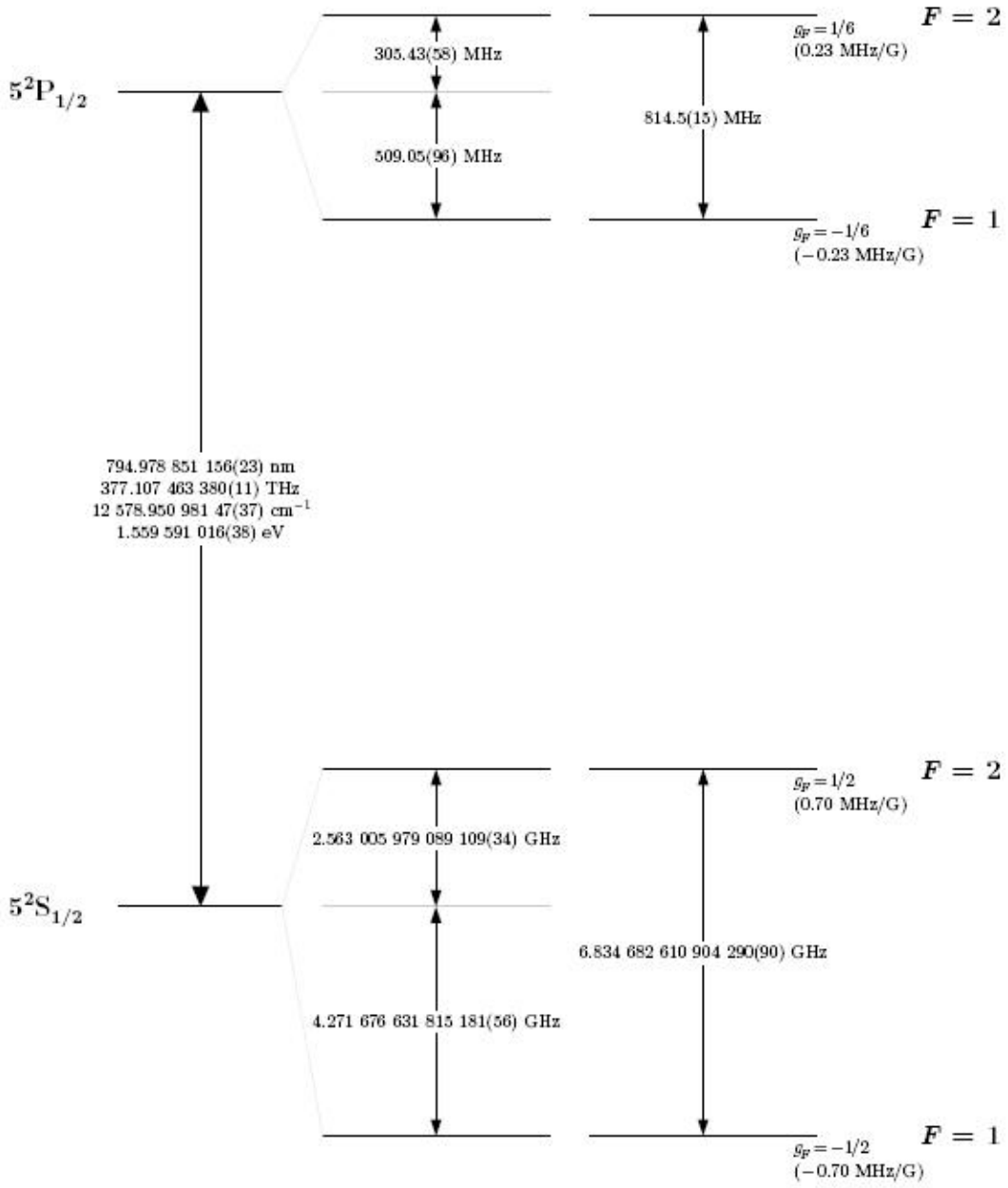

Figure A.1: Rb^{87} D_1 transition hyperfine structure. The frequency splitting due to hyperfine splitting are included. [13]

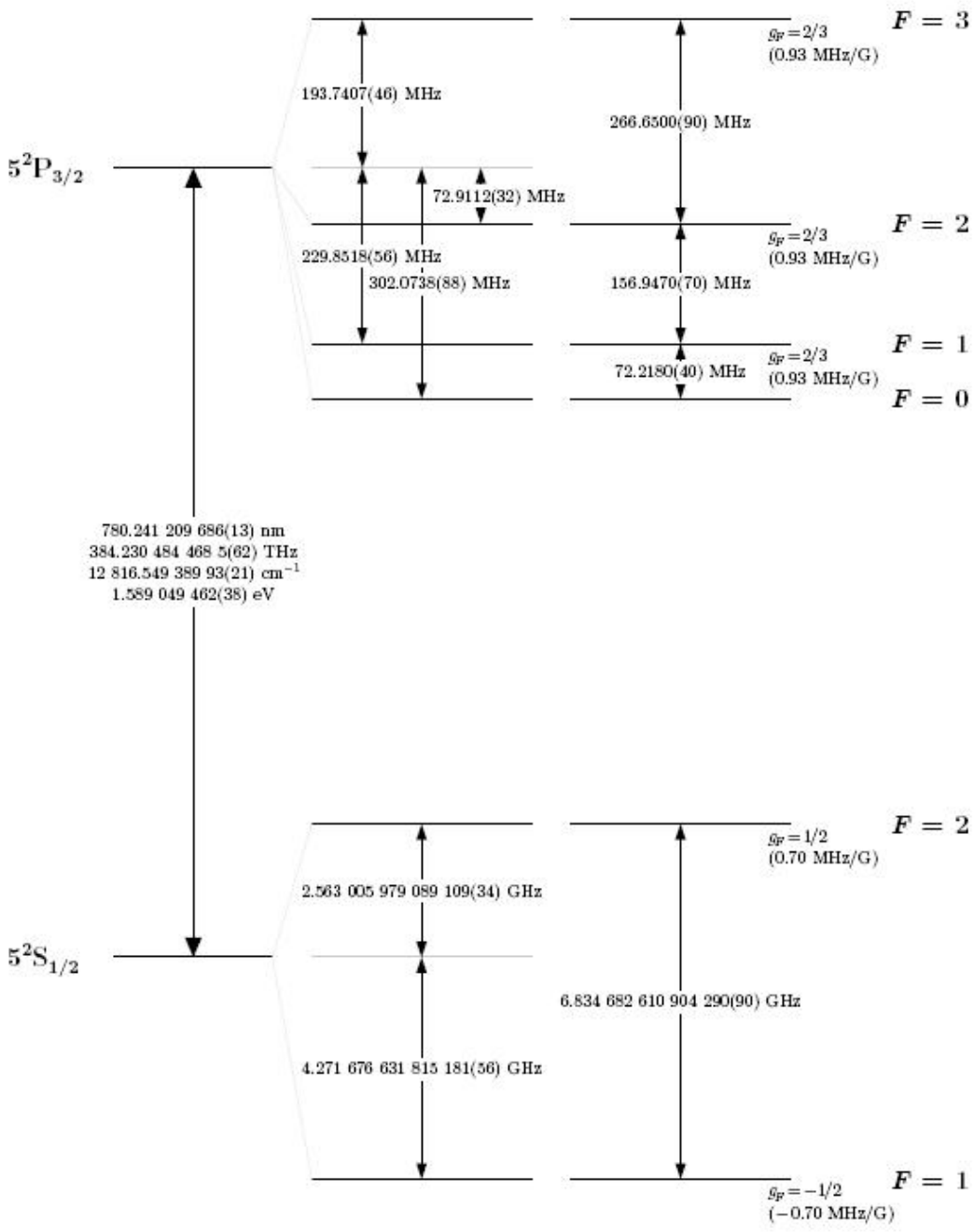

Figure A.2: Rb^{87} D_2 transition hyperfine structure. The frequency splitting due to hyperfine splitting are included. [13]

APPENDIX B

Diode laser locking

All diode lasers that are used to create the 2-D and 3D MOT have been frequency stabilized. The emission frequency of the laser strongly depends on its temperature, injection current, external optical cavity length and other parameters [27]. These parameters all contain noise. The most efficient way to reduce the noise is by locking the frequency to a reference frequency. The method used for locking the frequency of the lasers is a combination of saturation absorption spectroscopy and frequency modulation spectroscopy. The cooling laser beams need to be locked slightly red-detuned to the resonance frequency to make the optical force velocity dependent as is explained in Section 2.1. To do this a method called offset locking is used. All three methods will be explained in this section starting with saturation absorption spectroscopy.

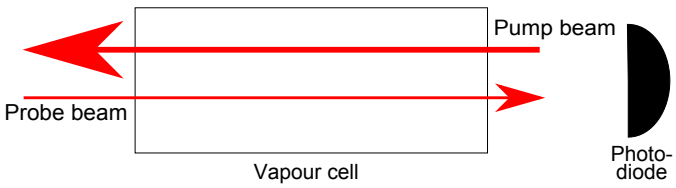

Figure B.1: Basic setup saturated absorption spectroscopy. The pump beam goes through the vapor cell and saturates the atomic transition. Afterwards the probe beam goes through the vapour cell. The intensity of the probe beam is then measured by a photodiode.

B.1 Saturation absorption spectroscopy

Saturation absorption spectroscopy, also called Doppler-free spectroscopy, is a method that enables precise determination of the transition frequency of the atoms between the ground states and excited states. The main problem in determining the transition frequency of the atoms is the occurrence of Doppler broadening. First the concept of Doppler broadening will be explained. After the concept is clear the solution to avoid Doppler broadening is presented, which is saturated absorption spectroscopy.

Normally the frequency distribution of a transition is highly broadened due to the Doppler effect. Atoms moving towards or away from the laser beam see the laser in their frame of reference with a different frequency. The atoms have a resonance frequency ν_0. If the atoms move with a velocity v the frequency at which atoms absorb a photon in the frame of the reference of the laser is

$$\nu_L = \nu_0 \left(1 + \frac{v}{c}\right), \tag{B.1}$$

with c being the speed of light. Thus atoms moving towards the laser will absorb photons from the laser that are blue-shifted ($\nu_L > \nu_0$), and atoms that move away from the laser absorb red-shifted photons ($\nu_L < \nu_0$). Therefore an ensemble of atoms having a distribution of velocities will absorb light over a range of frequencies. The result is a Doppler broadened frequency transition. The probability P that atoms in an atom cloud have a velocity between v and $v + dv$ is given by the Maxwell distribution [28]

$$P(v)dv = \left(\frac{M}{2\pi k_b T}\right)^{1/2} \exp\left(\frac{Mv^2}{2k_b T}\right) dv, \tag{B.2}$$

where M is the mass of the atom, T is the temperature, and k_b is the Boltzmann constant. The velocity of Equation B.1 can now be substituted in Equation B.2 to get the probability that the atoms absorb a photon with frequency between ν_L and $\nu_L + d\nu_L$

$$P(\nu_L)d\nu_L = \left(\frac{2}{\Gamma\pi^{1/2}}\right) \exp\left(\frac{-4(\nu_L - \nu_0)}{\Gamma^2}\right) d\nu_L. \tag{B.3}$$

The natural linewidth Γ is defined as

$$\Gamma \equiv \frac{2\nu_0}{c}\sqrt{\frac{2k_b T}{M}}. \tag{B.4}$$

The Doppler broadening causes individual spectral lines not to be resolved. The different transitions can not be seen clearly in a Doppler broadened spectrum. Therefore a method is generated that avoids the Doppler broadening of the spectral lines. To avoid Doppler broadening the atoms can be cooled to a temperature where Doppler broadening becomes irrelevant. However this is experimentally very difficult to realise. Saturation absorption spectroscopy uses a much easier and more practical method to avoid Doppler broadening.

Saturated absorption spectroscopy makes use of a pump-probe scheme. Part of the laser beam that is used in the experiment is split off for spectroscopy. This beam goes

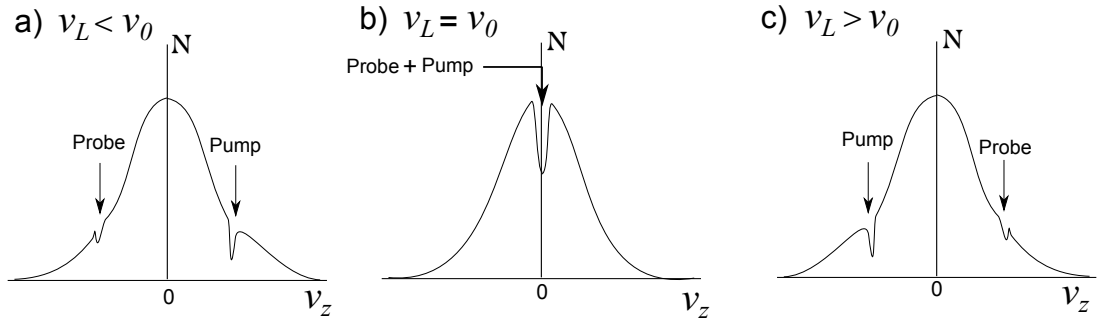

Figure B.2: Saturation absorption spectroscopy measurement. The number of photons that hit the photodiode (N) is measured for different frequencies (ν). a) The resonance frequency of the atoms is higher than the laser frequency. Atoms moving with a velocity towards the pump beam absorb photons of the laser, while atoms moving in the opposite direction towards the probe beam absorb photons from the probe beam. b) The laser frequency is equal to the resonance frequency of the atoms. Atoms with zero velocity in the direction on beam propagation absorb atoms of both beams. c) The resonance frequency of the atoms is lower than the laser frequency. Atoms moving with a velocity away from the pump beam absorb photons of the laser, while atoms moving in the opposite direction away from the probe beam absorb photons from the probe beam.

through a rubidium vapor glass cell pumping many atoms from the ground state to the excited state as depicted in Figure B.1. When the number of atoms in the ground state and excited state is approximately equal the transition is said to be saturated. The intensity of the pump beam is such that this saturation is reached. When saturation is reached the chance that an incoming photon excites an atom is much lower, as there are much less atoms in the ground state. The beam that passes the glass cell for the first time and saturates the atoms is called the pump beam. After going through the rubidium glass cell the beam is reflected by a mirror and goes back through the rubidium glass cell with velocity in the opposite direction. This beam moving in opposite direction is called the probe beam. This probe beam intensity is measured by a photodiode after going through the rubidium cell. When scanning across the frequency of the laser beam a narrow peak in the probe-beam signal at the resonance frequency will appear. The reason for this peak is the following. Only for atoms having zero velocity along the axis of beam propagation the two counterpropagating laser beams are seen at the same frequency. Atoms moving to the right see the pump beam blue-shifted and the probe beam red-shifted (Figure B.2 a), while atoms moving to the left see the pump beam red-shifted and the probe beam blue-shifted (Figure B.2 c). Atoms at zero velocity on the axis of propagation however do see both the pump and probe beam at the same frequency (Figure B.2 b). These atoms see no Doppler shift of the laser beam and will be excited at resonance frequency. The high intensity of the pump beam saturates the atoms with this velocity. This means most of these atoms will be in the excited state, and the ground state will be partially depleted. Now that the pump beam has saturated the transition the probe beam will encounter less atoms in the ground state to excite, and thus less intensity of the probe beam will be absorbed. When scanning along the frequency of the laser a small peak in the intensity of the probe beam will thus be encountered at the resonance frequency. This narrow peak has precisely determined the transition frequency. Wit this method Doppler broadening is avoided.

Apart from avoiding Doppler broadening of the spectrum, a further consequence of this method is the presence of cross-over lines. When two transitions are within a Doppler-broadened feature and have the same ground state, a crossover peak at the frequency exactly between the two transitions will be the result. The moving atoms see the pump and the probe beam resonant at separate transitions. For example if the frequency of the laser beam is exactly in between two transition frequencies of the atoms the pump beam will address the atoms moving with a velocity towards the beam. The probe beam can now also address these atoms that move away from the probe beam though at a different transition. The result is a small peak in intensity at the frequency exactly between two transitions. This peak is called the cross-over peak.

The result of saturation absorption spectroscopy is that we now have an absorption spectrum of all transition frequencies of rubidium. The frequency of the laser beams in the setup need to be locked on a number of these transitions. However locking on the peaks of the saturation absorption spectrum will not work. When locking on a peak a small deviation in frequency to either sides of the peak would give the same intensity deviation. Therefore a feedback mechanism is unable to correct for this, as it does not know to which side to correct. To be able lock on the transitions a second technique is used, which is frequency modulation spectroscopy.

B.2 Frequency modulation spectroscopy

Frequency modulation spectroscopy is a technique that converts a modulation in the frequency of the saturated absorption spectroscopy setup into an amplitude modulation. The technique is mainly based on the fact that a small modulation in the frequency at and around an absorption transition of the gas in the tube leads to a difference in absorption. The light intensity is therefore different, and this is measured by the photodiode. The frequency is modulated around the resonance frequency. The frequency modulation close to resonance causes an intensity modulation and this is measured. Far away from resonance there will be no absorption, and no changes in absorption, resulting in a flat line signal. Close to resonance however a strong intensity modulation will be measured. The frequency is locked on the slope of the intensity modulation signal. When there is a perturbation in the frequency signal, there is also a change in signal of the intensity modulated signal. Figure B.3 summarizes how frequency modulation spectroscopy works. As the frequency is locked on a slope, a small deviation to a higher frequency would give a different signal than a small deviation to a lower frequency. This signal of the frequency modulation spectrum is used as an error signal and send to a feedback mechanism, which makes sure the frequency stays in lock. Both the saturated absorption spectrum and the frequency modulated spectrum for natural rubidium are shown in Figure B.4. The black line represents the absorption of light at frequencies near the resonance frequency of the different transitions. The different transitions of both ^{85}Rb and ^{87}Rb give a dip in intensity as the photons are absorbed at and around the resonating frequency. The red line the frequency modulated signal is transformed into an intensity modulation. It immediately becomes clear from this graph that every

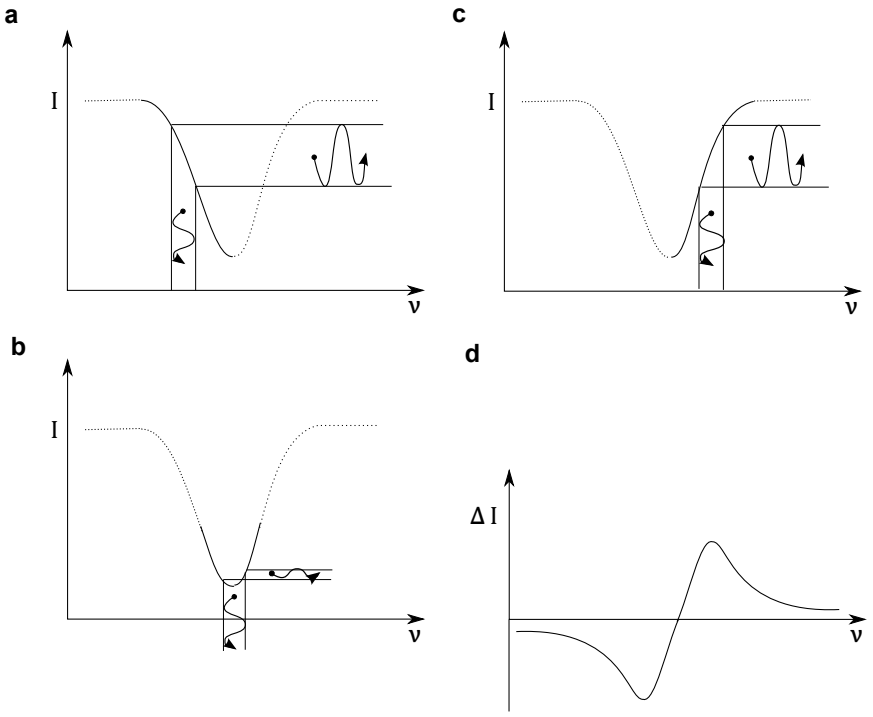

Figure B.3: In frequency modulation spectroscopy, as the frequency is scanned across the atomic transition, the the modulation in the frequency is converted into a modulation in amplitude. a) This gives rise to a modulation in the optical absorption of a sample at the same frequency. b,c) As you continue to scan across the absorption profile, you can see that the amount of FM to AM conversion varies. d) In the end the frequency modulation has been converted into an amplitude modulation. [29]

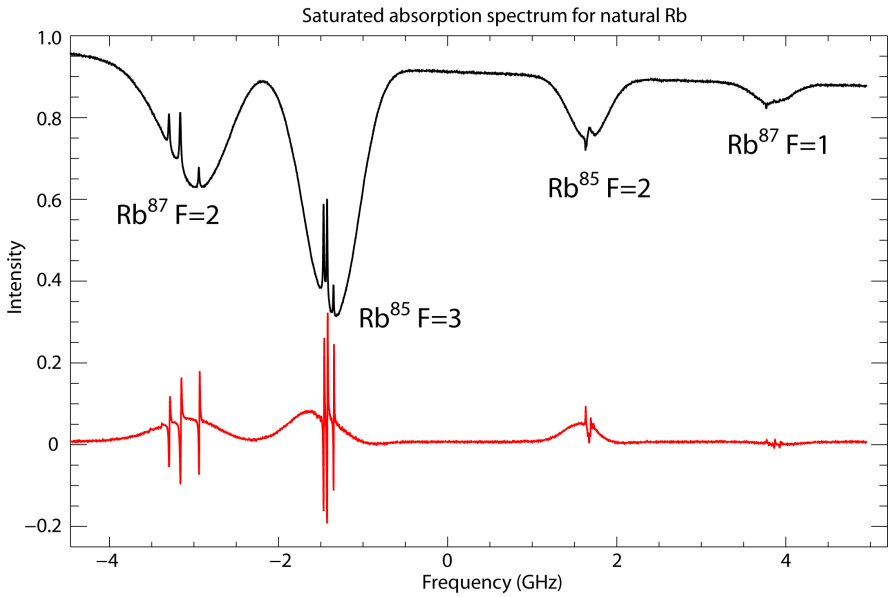

Figure B.4: Saturation absorption spectroscopy of rubidium. The black line represents the absorption at different frequencies. Both the ^{85}Rb and the ^{87}Rb transitions show a dip in the intensity profile. The red line shows how frequency modulation spectroscopy can transform the signal into an intensity modulation. The frequency is locked on the slopes of these peaks. [30]

transition has a number of peaks. These peaks represent both the hyperfine transitions and the crossover transitions. The cooling beam frequency needs to be locked slightly red-detuned to the resonance frequency in order to create a MOT. For this a technique called frequency offset locking is used.

B.3 Offset locking

To lock to a frequency slightly detuned to a transition frequency of rubidium a method called frequency offset locking is used. To form a MOT the frequency of the cooling lasers needs to be slightly red-detuned to the cooling transition frequency. The offset lock can do this in the following way.

Figure B.5 is a schematic representation of the offset lock. The frequency offset lock makes use of the frequency beat note of the cooling laser beam and the reference laser beam. The beat signal of two beams gives the sum and difference frequency signal of the two beams. The cooling beam and a reference beam are combined and focused on a photodiode. This photodiode superimposes the two signals and measures the frequency difference. The sum frequency signal is twice the optical frequency and way to fast to detect by a photodiode. The output signal $\Delta\nu = \nu_{\text{Cool}} - \nu_{\text{Ref}}$ is mixed with the output of a Direct Digital Synthesizer (DDS) frequency signal ν_{DDS}. This signal is split into two equal parts and then recombined by a mixer. A phase detector than measures the phase difference between the two signals. One part of the signal has been delayed by a

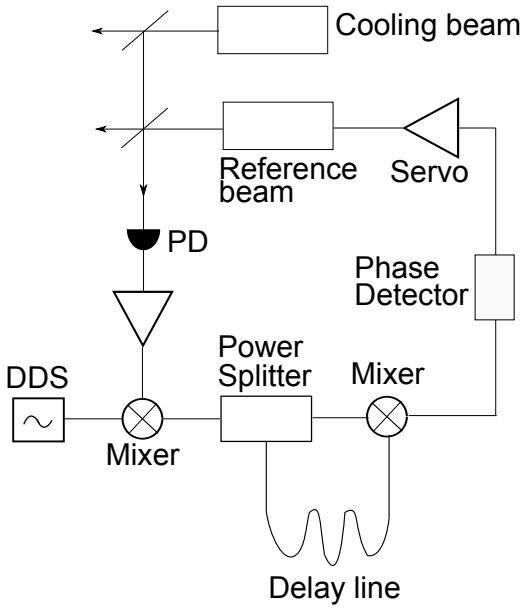

Figure B.5: Schematic representation of the offset locked.

long coax cable. The result due to the longer path of one of the two signals is a phase difference. The phase detector can then measure this phase difference as a function of beat frequency, resulting in a sinusoidal signal. The zero crossing of the signal provide the error signal for locking the difference frequency by using a servo loop. The circuit allows stable locking on several values of the beat frequency corresponding to the zero-crossings of the error signal. The DDS frequency signal ν_{DDS} can be used to change the position of the slopes. By now first locking the frequency of the reference laser beam ν_{Ref} and then locking on a beat frequency, the frequency of the cooling laser is locked at a detuning.

The reference laser is locked on the $(1, 3)$ cross-over transition that has been generated by the saturated absorption spectroscopy. Apart from being used as a reference beam part of this laser beam is split off and used for pushing the atoms from the 2-D to the 3-D MOT. Another part of the beam is used as a probe beam for doing absorption imaging measurements of the atoms in the ODT. The frequency of the part of the beam that is used for these purposes needs to be equal to the cooling transition frequency. The reason for this is that atoms then have the highest probability to absorb a photon. For the push beam this gives the highest probability of giving atoms a velocity towards the 3-D MOT. The probe beam of the ODT has the highest chance to absorb atoms when the frequency is on resonance with the transition frequency. As an absorption imaging technique is used to image the number of atoms in the ODT, the laser beam needs to be on the resonance transition. The difference frequency between the $(1, 3)$ transition and the $F = 2 \rightarrow F^{'} = 3$ cooling transition is 212 MHz [13]. The frequency of the reference beam can be changed by two acousto-optical modulators which can

change the frequency of the beam by around 80 or 120 Mhz each.

Bibliography

[1] Stockman M.I. 2011. Nanoplasmonics: past, present and glimpse into future. Optics Express 19, issue 22, pp. 22029-22106.

[2] Atwater, H.A., Polman, A. 2010. Plasmonics for improved photovoltaic devices. Nature materials 9, pp. 205-213.

[3] A.B. Dahlin. 2012. Plasmonic Biosensors: An Integrated View of Refractometric Detection. IOS Press. pp. 21.

[4] Atwater, H.A. 2007. The promise of plasmonics. Scientific American 4, pp. 56-63.

[5] Pan, L., Park, Y., Xiong, Y., Ulin-Avila, E., Wang, Y., Zeng, L., Xiong, S., Rho, J., Sun, C., Bogy, D.B., Zhang, X. 2011. Maskless plasmonic lithography at 22 nm resolution. Science Report 1, pp. 175.

[6] Greveling, S. 2013. Msc thesis: An optical dipole conveyor trap for Rubidium atoms.

[7] Kluit, Z. 2013. Msc thesis: A stereo-tweezer for ultracold atoms.

[8] Metcalf, H., van der Straten, P. 1994. Cooling and trapping of neutral atoms. Physics reports 244, pp.203-286.

[9] Raab, E., Prentiss, M., Cable, A., Chu, S., Pritchard,d. Trapping of neutral sodium atoms with radiation pressure, Physical Review Letters 59, pp. 2631.

[10] Grimm, R., Weidemuller, M., Ovchinniikov, Y.B. 2000. Optical dipole traps for neutral atoms. Advances in Atomic, Molecular, and Optical Physics 42, pp. 95.

[11] Phillips, W.D., 1997. Laser cooling and trapping of neutral atoms. Nobel Lecture.

[12] Kowalski, K., Cao Long, V., Dinh Xuan, K., Glodz, M., Nguyen Huy, B., Szonert, J. 2010. Magneto-optical trap: Fundamentals and realization. Computational methods in science and technology, special issue 2, pp.115-129.

[13] Steck, D.A. 2001. Rubidium 87 D-line data.

[14] Sakurai, J.J. 1994. Modern quantum mechanics. Addison-Wesley Publishing company.

[15] Silfvast, W.T. 2004. Laser fundamentals. Cambridge university press.

[16] Allen, L., and Eberly, J.H. 1975. Optical resonance and two-level atoms (Wiley, New York).

[17] Dalibard, J., Cohen-Tannoudji, C. 1985. Dressed-atom approach to atomic motion in laser light: the dipole force revisited. Journal of the optical society of America 2. pp. 1707-1720.

[18] Hess, H.f., Kochanski, G.P., Doyle, J.M., Masuhara, N., Kleppner, D., and Greytak, T.J. 1987. Physical Review Letters 59, pp. 672.

[19] Adams, C.S., Lee, H.J., Davidson, N., Kasevich, M., Chu, S. 1995. Evaporative cooling in a crossed beam trap. Physical Review Letters 74. pp. 3577-3580.

[20] Verboven, T. 2013. Bsc thesis: Magneto-optical trap optimalization.

[21] Gillen, G.D., Seck, C.M., Guha, S. 2010. Analytical beam propagation model for clipped focused-Gaussian beams using vector diffraction theory. Optics Express vol. 18, no.5 pp. 4023-4040.

[22] Griffiths, D.J., 2005. Introduction to Quantum Mechanics. Pearson Education, Inc.

[23] Drewsen, M., Laurent, P., Nadir, A., Santarelli, G., Clairon, A., Castin, Y., Grison, D., and Salomon, C. (1994). Applied Physics B 59, pp. 283.

[24] Yang, L., Han, B., Hong, D., Mohamed, T.A., Han, D.J. 2007. Loading and compression of a large number of Rubidium atoms using a semi-dark type magneto-optical trap. Chinese journal of physics 46. pp. 606-615.

[25] Karssen, L. 2008. Phd thesis: Trapping cold atoms with ultrashort laser pulses.

[26] Arnold, K.J., Barrett, M.D. 2011. All-optical Bose-Einstein condensation in a 1.06 micron dipole trap. Optics communications 284, pp. 3288-3291.

[27] Sargsyan, A., Papoyan, A.V., Sakisyan, D., Weis, A. 2009. Efficeint technique for measuring laser frequency stability. European physical Journal - Applied Physics 48. pp. 1-5.

[28] Blundell, S.J., Blundell, K.M. 2008. Concepts in thermal physics. Oxford University press

[29] Newport.

[30] Moglabs.